2.3. Calculation of m values

To analyze the effects of alcohols on AGP, we assumed a two-state transition between the β-sheet and the α-helix states. The equilibrium constant for the conformational transition, K, is defined as $K = [H]/[B]$, where [H] and [B] are the concentrations of the α-helix and β-sheet states, respectively. The free energy change (ΔG_f) for formation of the helical state is calculated according to following equation:

$$\Delta G_f = -RT \ln K,$$

where R is the gas constant, and T is the temperature in Kelvin. We assumed a linear dependence of ΔG_f upon the alcohol concentration ([alcohol]):

$$\Delta G_f = \Delta G_0 - m[\text{alcohol}],$$

where ΔG_0 is the ΔG_f value in the absence of alcohol, and m is a measure of the dependence of ΔG_f on the concentration of alcohol.

Least squares curve fitting was done using the MULTI program [28]. The solvent-accessible surface areas (total ASA [ASA (T)], hydrophobic ASA [ASA (H)], negative charge ASA [ASA (N)], and positive charge ASA [ASA (P)]) of alcohols were estimated using the Molecular Operating Environment (Chemical Computing Group Inc., Canada). ASA (H)/ASA (T), ASA (N)/ASA (T) and ASA (P)/ASA (T) were represented as relative ASA (H) [rASA (H)], relative ASA (N) [rASA (N)] and relative ASA (P) [rASA (P)], respectively (see Table 1).

3. Results

3.1. Effects of alkanols on α-helix formation in AGP

Based on a previous report that 40% methanol can induce α-helix formation at pH 4.0 [22], we investigated the effect of hydrocarbon groups in alcohols on the structure of AGP (Fig. 1A). The $[\theta]$ value at 222 nm, an index of α-helix content, showed saturation at lower concentrations as the alkyl chain length was increased. This demonstrated that the capacity to induce α-helix formation was increased as the hydrocarbon chain length was increased. However, there did not seem to be a difference in the effects of various alkanols on the α-helix content of AGP. Furthermore, 1-propanol, which has a straight chain, was more effective in promoting α-helix formation than 2-propanol, which has a branched chain.

3.2. Effects of diols on α-helix formation in AGP

Next, to determine the role of the hydroxyl group, we examined the effects of several diols on the α-helix content. As in the case of the alkanols, transition to an α-helix structure was observed at lower concentrations as the chain length was increased (Fig. 1B). However, the effect was weaker than in the case of the alkanols. This result suggests that the hydroxyl group of the alcohol only plays a role in their dissolution in water and that the induction of α-helix formation is due to the hydrocarbon moiety.

3.3. Effects of halogenols on α-helix formation in AGP

In addition, we examined the effect of halogen moieties by using several halogenols (Fig. 1C). The $[\theta]$ value at 222 nm in 2-chloroethanol (ClEtOH) showed the transition and saturation at lower concentrations than for the alkanols and diols, and caused a remarkable increase in the α-helix content. In contrast, the effect of 2-fluoroethanol (FEtOH) was weaker than that of ethanol. Bromoethanol could not be used because of phase separation. Alternatively, 2,2,2-trifluoroethanol (TFE) and 1,1,1,3,3,3-hexafluoro-2-ethanol (HFIP) was used. It was observed that these alcohols strongly promote an α-helix formation in AGP. These results imply that the presence of multiple F atoms increases the effectiveness markedly, although the F atom itself is not so potent and halogen atoms markedly increase the ability of the solvent to induce α-helix formation in AGP.

3.4. Effects of hydrophobic force and negative charge on α-helix formation in AGP

Based on the findings with various alcohols, it appeared likely that the hydrophobicity and negative charge of the alcohol participate in the induction of α-helix formation in AGP. Thus, we estimated rASA (H), rASA (P), and rASA (N), respectively, which do not depend on the molecular weight or ASA (T), to evaluate the properties of the alcohols. The effects of the alcohols on AGP were evaluated using with the m value and the α-helix effect$_{50}$ (HE_{50}), which is the concentration (%) resulting in a 50% transition from a β-sheet to an α-helix. For all kinds of alcohols, HE_{50} appears to more accurately describe the effects of the alcohol than the m value because the m value depends on maximum α-helix content. In Fig. 2, correlations between HE_{50} and rASA were presented. In alkanols, a good correlation was observed between the HE_{50} and rASA (H) ($r = 0.8849$), suggesting that hydrophobic interactions are involved in α-helix formation in AGP at pH

Table 1
The m, HE_{50}, rASA (H), rASA (N) and rASA (P) values for various alcohols

	Abbreviation used	m (J mol^{-1} M^{-1})	HE_{50}	rASA (H)	rASA (N)	rASA (P)
Alkanols						
Methanol	MeOH	573.7	35.1	0.41	0.17	0.42
Ethanol	EtOH	751.1	28.8	0.67	0.11	0.21
1-Propanol	1-PrOH	952.2	21.8	0.72	0.10	0.17
2-Propanol	2-PrOH	789.8	25.7	0.78	0.09	0.12
Diols						
1,2-Ethanediol	1,2-Et(OH)$_2$	328.9	67.4	0.42	0.21	0.38
1,2-Propanediol	1,2-Pr(OH)$_2$	381.2	54.5	0.58	0.17	0.25
1,4-Butanediol	1,4-Bu(OH)$_2$	393.2	49.3	0.64	0.12	0.24
2,3-Butanediol	2,3-Bu(OH)$_2$	469.5	51.3	0.68	0.13	0.18
Halogenols						
2-Fluoroethanol	FEtOH	625.7	37.1	0.43	0.28	0.28
2-Chloroethanol	ClEtOH	397.4	26.6	0.38	0.42	0.20
2,2,2-Trifluoroethanol	TFE	545.3	23.1	0.20	0.60	0.20
1,1,1,3,3,3-Hexafluoro-2-propanol	HFIP	1004.9	5.8	0.07	0.79	0.12

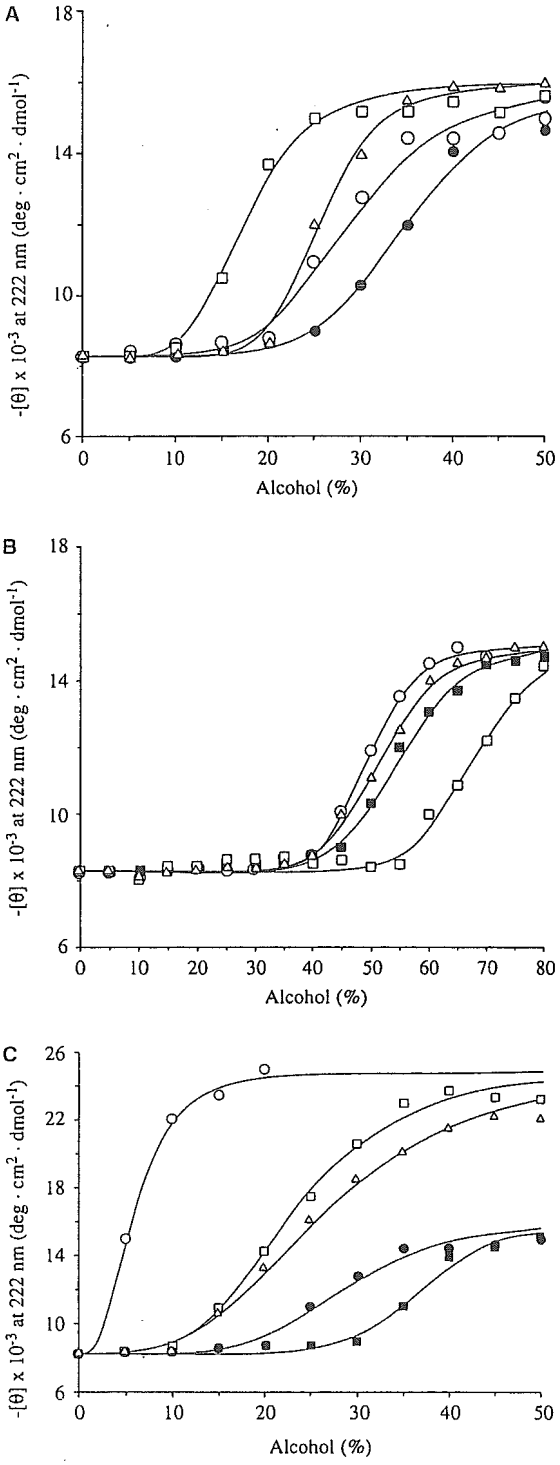

Fig. 1. Effects of alkanols (A), diols (B), and halogenols (C) on α-helix formation in AGP. The α-helix content of AGP was monitored at pH 4.0 by measuring the ellipticity at 222 nm. Abbreviations are as follows: in panel A, MeOH (●), EtOH (○), 1-PrOH (□), and 2-PrOH (△); in panel B, $Et(OH)_2$ (□), $1,2\text{-}Pr(OH)_2$ (■), $2,3\text{-}Bu(OH)_2$ (△), and $1,4\text{-}Bu(OH)_2$ (○); and in panel C, EtOH (●), FEtOH (■), ClEtOH (△), TFE (□), and HFIP (○). The lines were drawn using the MULTI program [28].

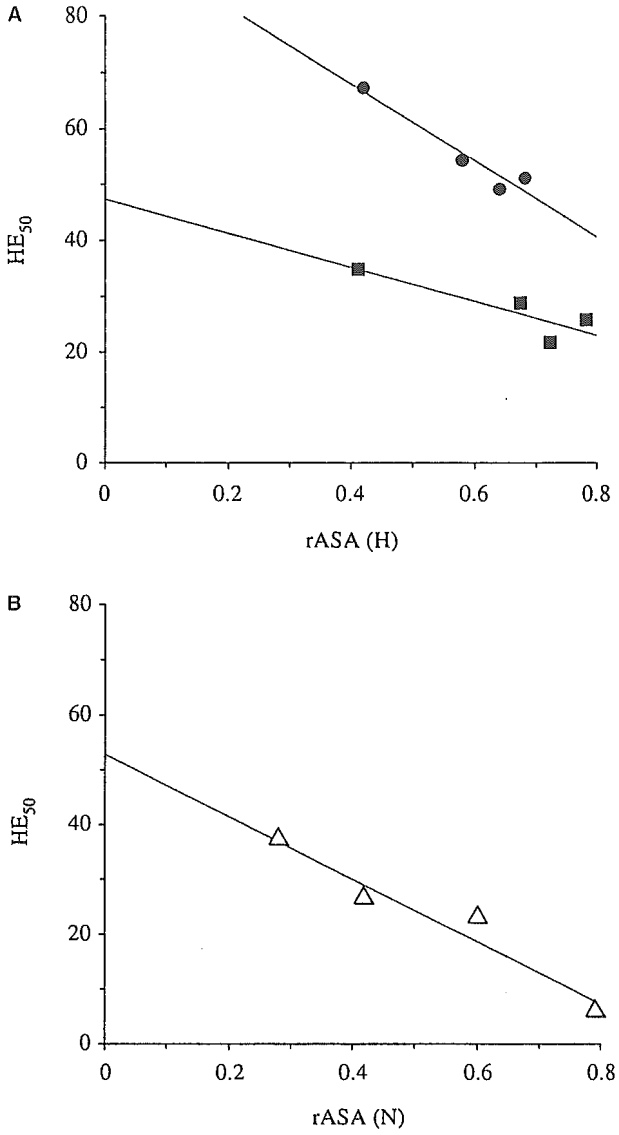

Fig. 2. Correlations between the values of HE_{50} and rASA. A and B show the correlations between HE_{50} and rASA (H) or rASA (N), respectively. Each symbol represented as follow: alkanol (●), diol (■) and halogenol (△).

4.0 (Fig. 2A). For diols, rASA (H) showed significant correlations with the HE_{50} ($r = 0.9685$, $P < 0.05$). This result also indicates that hydrocarbon group contributes to α-helix formation in AGP, although the effect itself was weaker than that of alkanols (Fig. 2A). On the other hand, for halogenols we found a significant correlation between HE_{50} and rASA (N) ($r = 0.9702$, $P < 0.05$), which explains the strong effect of the negative charge on α-helix formation in AGP (Fig. 2B).

3.5. Effect of halogen (Cl^-) on α-helix formation in AGP

The significant correlation between HE_{50} and rASA (N) in halogenols indicates that halogen is an important factor in the induction of α-helix formation in AGP. Previously, we reported that NaCl (1 M) induced an α-helix structure at pH 2.0 [12]. To examine the effect of the halogen, Cl^-, on the α-helix formation, CD spectra was monitored in the presence of HCl and NaCl (0–1 M) at pH 2.0 (Fig. 3). Interestingly, addition of HCl induced the α-helix structure, although AGP was in an unfolded state at pH 2.0. Moreover, NaCl also showed a significant ability to induce α-helix formation. These results suggested that halogen is a key factor in the induction of α-helix

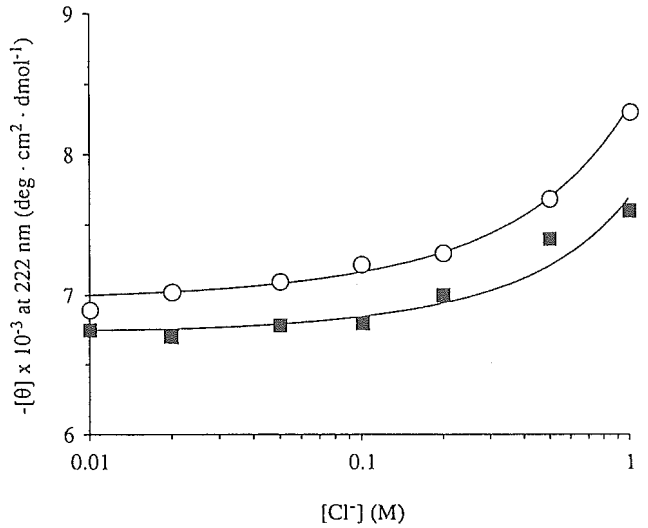

Fig. 3. Effect of halogen (Cl^-) on α-helix formation in AGP. The α-helix content of AGP was monitored at pH 2.0 by measuring the ellipticity at 222 nm. Abbreviations are as follows: ○, NaCl; and ■, HCl. The lines were drawn using the MULTI program [28].

formation by halogenols and that negative charge acts cooperatively with hydrophobicity to induce α-helix structure formation.

4. Discussion

Previously, we reported that AGP interacts with biomembrane models, including liposomes and reverse micelles, and that this interaction is followed by conformational transition from a β-sheet form to an α-helix form [12,13]. This conformational transition may be linked not only to ligand-binding capacity but also to intracellular biological activity [29–33], but which factors participate in such a conformational transition has not been determined. Generally, it has been thought that following factors are related to the interaction between proteins and lipid membranes: (1) negative charge of the membrane surface; (2) a mild acidic environment on the membrane surface and (3) a hydrophobic membrane interior [17]. However, it is difficult to evaluate the role of these factors in the conformational transition using liposomes and reverse micelles separately.

In the present study, to clarify the mechanism by which AGP undergoes a transition from an α-helix to a β-sheet structure, we examined the effects of various alcohols. Both Alkanol and diol showed larger values of rASA (H) than rASA (N) and rASA (P) and the abilities of alkanols and diols to induce formation of an α-helix structure were dependent on the length of their hydrocarbon groups. These HE_{50} values correlated well with the rASA (H). These results indicate that hydrophobic force is a key factor for inducing and stabilizing the α-helix structure. The effects of diols were weaker than other alcohols because the hydroxyl group weakened the hydrophobicity. On the other hand, the HE_{50} values of halogenols correlated significantly with the rASA (N), implying that the α-helix formation in the presence of alcohols is due to the cooperative action of hydrophobic and electrostatic forces. The strong effect of halogenols may be due to their high rASA (N). This hypothesis is also supported by the finding that HCl and NaCl induced α-helix formation in AGP even at pH 2.0. Under acidic conditions, it appears that hydrophobic interaction between the hydrocarbon group of the alcohol and the exposed hydrophobic region of AGP induces formation of the α-helix structure. Kodicek et al. [27] reported that AGP formed a similar α-helix structure in the presence of MeOH at high temperature. We also found that the conformational structure of AGP perturbed at high temperature (data not shown). In addition, suppression of the electrostatic repulsion of positive charges in AGP by the negative charge of the halogen might enhance the hydrophobic interaction. Although HCl and NaCl also induced α-helix formation, the effect was weaker than that of alcohols. These results indicate that there is a slight increase in the extent of α-helix conformation when AGP interacts with the membrane surface, and then the peptide inserts into the membrane interior, where it forms an α-helix-rich structure.

In the present study, we found that hydrophobic and electrostatic forces cooperatively promote α-helix formation in AGP. The biological function of AGP is not clear, but some reports suggest that it has intracellular activities [29–33]. Given that AGP is a plasma protein, the conformational transition to an α-helix structure may be critical for its activity.

References

[1] Treuheit, M.J., Costello, C.E. and Halsall, H.B. (1992) Analysis of the five glycosylation sites of human alpha1-acid glycoprotein. Biochem. J. 283, 105–112.
[2] Halsall, H.B., Austin, R.C., Dage, J.L., Sun, H. and Schlueter, K.T. (2000) Structural aspects of alpha1-acid glycoprotein and its interaction in: Proceedings of the International Symposium on Serum Albumin and Alpha1-acid Glycoprotein (Otagiri, M., Sugiyama, Y., Testa, B. and Tillement, J.P., Eds.), pp. 45–54, Tokyo Print, Kumamoto, Japan.
[3] Kremer, J.M., Wilting, J. and Janssen, L.H. (1988) Drug binding to human alpha1-acid glycoprotein in health and disease. Pharmacol. Rev. 40, 1–47.
[4] Baumann, P., Muller, W.E., Eap, C.B. and Tillement, J.P. (1989) Alpha1-acid Glycoprotein. Genetics, Biochemistry, Physiological Functions and Pharmacology, Alan R. Liss Inc., New York.
[5] Israili, Z.H. and Dayton, P.G. (2001) Human alpha1-glycoprotein and its interactions with drugs. Drug Metab. Rev. 33, 161–235.
[6] Aubert, J.P. and Loucheux-Lefebvre, M.H. (1976) Conformational study of alpha1-acid glycoprotein. Arch. Biochem. Biophys. 175, 400–409.
[7] Rojo-Dominguez, A. and Hernandez-Arana, A. (1993) Three-dimensional modeling of the protein moiety of human alpha1-acid glycoprotein, a lipocalin-family member. Protein Seq. Data Anal. 5, 349–355.
[8] Lin, T.H., Sawada, Y., Sugiyama, Y., Iga, T. and Hanano, M. (1987) Effects of albumin and alpha1-acid glycoprotein on the transport of imipramine and desipramine through the blood–brain barrier in rats. Chem. Pharm. Bull. 35, 294–301.
[9] Forker, E.L. and Luxon, B.A. (1981) Albumin helps mediate removal of taurocholate by rat liver. J. Clin. Invest. 67, 1517–1522.
[10] Weisiger, R., Gollan, J. and Ockner, R. (1981) Receptor for albumin on the liver cell surface may mediate uptake of fatty acids and other albumin-bound substances. Science 211, 1048–1051.
[11] Forker, E.L. and Luxon, B.A. (1983) Albumin-mediated transport of rose bengal by perfused rat liver. Kinetics of the reaction at the cell surface. J. Clin. Invest. 72, 1764–1771.
[12] Nishi, K., Sakai, N., Komine, Y., Maruyama, T., Halsall, H.B. and Otagiri, M. (2002) Structural and drug-binding properties of alpha1-acid glycoprotein in reverse micelles. Biochim. Biophys. Acta 1601, 185–191.
[13] Nishi, K., Maruyama, T., Halsall, H.B., Handa, T. and Otagiri, M. (2004) Binding of alpha1-acid glycoprotein to membrane

results in a unique structural change and ligand release. Biochemistry 43, 10513–10519.
[14] Cheresh, D.A., Haynes, D.H. and Distasio, J.A. (1984) Interaction of an acute phase reactant, alpha1-acid glycoprotein (orosomucoid), with the lymphoid cell surface: a model for non-specific immune suppression. Immunology 51, 541–548.
[15] Neitchev, V.Z. and Bideaud, F.A. (1988) Temperature-dependent osmotic permeability in glycoprotein containing liposomes. Mol. Biol. Rep. 13, 85–88.
[16] van der Goot, F.G., Gonzalez-Manas, J.M., Lakey, J.H. and Pattus, F. (1991) A 'molten-globule' membrane-insertion intermediate of the pore-forming domain of colicin A. Nature 354, 408–410.
[17] McLaughlin, S. (1989) The electrostatic properties of membranes. Annu. Rev. Biophys. Biophys. Chem. 18, 113–136.
[18] Bychkova, V.E., Berni, R., Rossi, G.L., Kutyshenko, V.P. and Ptitsyn, O.B. (1992) Retinol-binding protein is in the molten globule state at low pH. Biochemistry 31, 7566–7571.
[19] Suren, A.T. and Lukas, K.T. (1996) Reversible pH-dependent conformational change of reconstituted influenza hemagglutinin. J. Mol. Biol. 260, 312–316.
[20] Jeffrey, P.D., Bewley, M.C., MacGillivray, R.T., Mason, A.B., Woodworth, R.C. and Baker, E.N. (1998) Ligand-induced conformational change in transferrins: crystal structure of the open form of the N-terminal half-molecule of human transferrin. Biochemistry 37, 13978–13986.
[21] Gasymov, O.K., Abduragimov, A.R., Yusifov, T.N. and Glasgow, B.J. (1998) Structural changes in human tear lipocalins associated with lipid binding. Biochim. Biophys. Acta 1386, 145–156.
[22] Bychkova, V.E., Dujsekina, A.E., Klenin, S.I., Tiktopulo, E.I., Uversky, V.N. and Ptitsyn, O.B. (1996) Molten globule-like state of cytochrome *c* under conditions simulating those near the membrane surface. Biochemistry 35, 6058–6063.
[23] Sonnichsen, F.D., Van Eyk, J.E., Hodges, R.S. and Sykes, B.D. (1992) Effect of trifluoroethanol on protein secondary structure: an NMR and CD study using a synthetic actin peptide. Biochemistry 31, 8790–8798.
[24] Yang, J.J., Buck, M., Pitkeathly, M., Kotik, M., Haynie, D.T., Dobson, C.M. and Radford, S.E. (1995) Conformational properties of four peptides spanning the sequence of hen lysozyme. J. Mol. Biol. 252, 483–491.
[25] Hamada, D., Kuroda, Y., Kataoka, M., Aimoto, S., Yoshimura, T. and Goto, Y. (1996) Role of heme axial ligands in the conformational stability of the native and molten globule states of horse cytochrome *c*. J. Mol. Biol. 256, 172–186.
[26] Kuroda, Y., Hamada, D., Tanaka, T. and Goto, Y. (1996) High helicity of peptide fragments corresponding to beta-strand regions of beta-lactoglobulin observed by 2D-NMR spectroscopy. Fold. Des. 1, 255–263.
[27] Kodicek, M., Infanzon, A. and Karpenko, V. (1995) Heat denaturation of human orosomucoid in water/methanol mixtures. Biochim. Biophys. Acta 1246, 10–16.
[28] Yamaoka, K., Tanigawara, Y., Nakagawa, T. and Uno, T. (1981) A pharmacokinetic analysis program (multi) for microcomputer. J. Pharmacobiodyn. 4, 879–885.
[29] van Molle, W., Denecker, G., Rodriguez, I., Brouckaert, P., Vandenabeele, P. and Libert, C. (1999) Activation of caspases in lethal experimental hepatitis and prevention by acute phase proteins. J. Immunol. 163, 5235–5241.
[30] Daemen, M.A., Heemskerk, V.H., van't Veer, C., Denecker, G., Wolfs, T.G., Vandenabeele, P. and Buurman, W.A. (2000) Functional protection by acute phase proteins alpha1-acid glycoprotein and alpha1-antitrypsin against ischemia/reperfusion injury by preventing apoptosis and inflammation. Circulation 102, 1420–1426.
[31] Hochepied, T., Van Molle, W., Berger, F.G., Baumann, H. and Libert, C. (2000) Involvement of the acute phase protein alpha1-acid glycoprotein in nonspecific resistance to a lethal gram-negative infection. J. Biol. Chem. 275, 14903–14909.
[32] Hochepied, T., Berger, F.G., Baumann, H. and Libert, C. (2003) Alpha1-acid glycoprotein: an acute phase protein with inflammatory and immunomodulating properties. Cytokine Growth Factor Rev. 14, 25–34.
[33] de Vries, B., Walter, S.J., Wolfs, T.G., Hochepied, T., Rabina, J., Heeringa, P., Parkkinen, J., Libert, C. and Buurman, A. (2004) Exogenous alpha1-acid glycoprotein protects against renal ischemia-reperfusion injury by inhibition of inflammation and apoptosis. Transplantation 78, 1116–1124.

0022-3565/05/3142-932-938$20.00
THE JOURNAL OF PHARMACOLOGY AND EXPERIMENTAL THERAPEUTICS
Copyright © 2005 by The American Society for Pharmacology and Experimental Therapeutics
JPET 314:932-938, 2005

Vol. 314, No. 2
85613/3041880
Printed in U.S.A.

Renal Clearance of Endogenous Hippurate Correlates with Expression Levels of Renal Organic Anion Transporters in Uremic Rats

Tsuneo Deguchi, Mizue Takemoto, Nao Uehara, W. Edward Lindup, Ayaka Suenaga, and Masaki Otagiri

Department of Biopharmaceutics, Graduate School of Pharmaceutical Sciences, Kumamoto University, Kumamoto, Japan (T.D., M.T., N.U., A.S., M.O.); and Department of Pharmacology and Therapeutics, University of Liverpool, Liverpool, England (W.E.L.)

Received March 1, 2005; accepted May 2, 2005

ABSTRACT

Hippurate (HA) is a harmful uremic toxin that accumulates during chronic renal failure, and failure of the excretion system for uremic toxins is thought to be responsible. Recently, we reported that rat organic anion transporter 1 (rOat1) is the primary mediator of HA uptake in the kidney, and so now we have studied the pharmacokinetics and tissue distribution of HA after a single i.v. dose of HA to normal and 5/6 nephrectomized rats (5/6Nx rats). In control rats, the renal and biliary clearances of HA were 18.1 and 0.1 ml/min/kg, respectively. Plasma clearance decreased as dosage increased from 0.1 to 5 mg/kg, which suggests that renal tubular secretion is the primary route for elimination of HA. The plasma clearance of HA was significantly decreased in 5/6 Nx rats compared with normal rats. In 5/6 Nx rats, renal clearance of endogenous HA correlated more closely with clearance of *p*-aminohippurate than with that of creatinine. Protein expression of rOat1 and rOat3, assessed by Western blot analysis, was decreased in 5/6 Nx rats. Furthermore, in 5/6 Nx rats, the renal secretory clearance of endogenous HA correlated closely with protein expression of renal rOats. Thus, HA is primarily eliminated from the plasma via the kidney by active tubular secretion. The renal clearance of endogenous HA seems to be a useful indicator of changes in renal secretion that accompany the reduced levels of OAT protein in chronic renal failure.

In chronic renal failure (CRF) patients, uremic toxins accumulate in the serum because of impaired renal clearance (Niwa, 1996). Serum levels of the uremic toxin hippurate (HA) are markedly elevated in patients with uremia (Vanholder et al., 2003). It has been suggested that HA plays a role in a variety of pathological conditions, including stimulation of ammoniagenesis (Dzurik et al., 2001), and inhibition of both plasma protein binding (Sakai et al., 1995) and organic anion secretion by the kidney (Boumendil-Podevin et al., 1975). HA also inhibits glucose utilization in muscles and so may be involved in development of muscular weakness in uremia (Spustova et al., 1987, 1989). Serum and cerebrospinal fluid concentrations of HA correlate positively with neurophysiological indices (Schoots et al., 1989), which suggests that HA induces neurological symptoms, perhaps via inhibition of organic anion transport at the blood-brain barrier (Ohtsuki et al., 2002) or blood-cerebrospinal fluid barrier (Porter et al., 1975). In addition, HA accelerates the renal damage associated with CRF (Satoh et al., 2003). Thus, HA can be classified as a uremic toxin and is consequently a compound of pharmacological interest.

Despite the important role of HA in the pathophysiology of uremia, little information is available regarding its pharmacokinetics in animals, and no studies of its tissue distribution have been reported. HA is the glycine conjugate of benzoate, which is formed primarily from aromatic amino acids by gastrointestinal flora and is added to foods and beverages as a preservative (Niwa, 1996). Active tubular secretion is the primary route for elimination of HA from the plasma via the kidney, and functional failure of this system causes accumulation of HA in blood (Tsutsumi et al., 2002). Recently, we reported that rat organic anion transporter 1 (rOat1) plays a major role in the renal uptake of HA on the basolateral

This work was supported, in part, by the Sasakawa Scientific Research Grant from The Japan Science Society.
Article, publication date, and citation information can be found at http://jpet.aspetjournals.org.
doi:10.1124/jpet.105.085613.

ABBREVIATIONS: CRF, chronic renal failure; HA, hippurate; 5/6 Nx rats, 5/6 nephrectomized rats; rOat, rat organic anion transporter; OAT, organic anion transporter; PAH, *p*-aminohippuric acid; BUN, blood urea nitrogen; HPLC, high-performance liquid chromatography; GFR, glomerular filtration rate; TBS-T, Tris-buffered saline/Tween 20; OCT, organic cation transporter; hOAT1, human organic anion transporter 1.

membrane of the proximal tubules (Deguchi et al., 2004). Also, there is evidence that HA inhibits OAT1- or OAT3-mediated transport in predialysis patients, leading to acceleration of serum accumulation of uremic toxins and reduction of plasma elimination of drugs via OAT1 and OAT3. The distribution and accumulation of HA in various tissues seems to be an important step in the development of uremic toxicity in renal failure. Therefore, it is important to clarify the changes in HA pharmacokinetics that occur in uremia.

To investigate the mechanisms of uremic symptoms and pharmacokinetics of HA, we conducted the present pharmacokinetic study, in which normal and 5/6 nephrectomized (5/6 Nx) rats received a single i.v. administration of HA. We also examined the renal and biliary excretion of HA after i.v. administration of HA to anesthetized rats and examined tissue distribution of endogenous HA. Additionally, we evaluated the suitability of HA clearance as a clinical marker of renal function.

Materials and Methods

Materials. [^{14}C]HA (55.0 mCi/mmol), [^{14}C]carboxyl-inulin (2.0 mCi/g), and [^{3}H]inulin (1.03 mCi/g) were purchased from American Radiolabeled Chemicals (St. Louis, MO). [^{3}H]*p*-Aminohippurate (PAH) (4.54 Ci/mmol) was purchased from PerkinElmer Life and Analytical Sciences (Boston, MA). HA was obtained from Sigma-Aldrich (St. Louis, MO). PAH was obtained from Nacalai Tesque (Kyoto, Japan). Polyclonal antibodies for rOat1 and rOat3 were purchased from Trans Genic Inc. (Kumamoto, Japan). Polyclonal antibody for Na^+-K^+ ATPase was purchased from Upstate Biotechnology (Lake Placid, NY). All chemicals were of analytical grade.

Animals. Adult male Wistar rats were housed in an air-conditioned room with free access to commercial feed and water and fasted for 16 h before experiments. All animal experiments were conducted according to the guidelines of Kumamoto University for the care and use of laboratory animals.

Induction of CRF by Surgical Reduction of Renal Mass. Experimental CRF was induced by 5/6 Nx (Deguchi et al., 2003). Male Wistar rats (130–150 g) were anesthetized with sodium pentobarbital (60 mg/kg) by intraperitoneal injection. During surgery, the body temperature of the rats was maintained using a warming lamp. The left kidney was exposed via a left flank incision and was gently dissected free from the adrenal gland, followed by excision of the upper and lower poles. One week later, the rats were again anesthetized with sodium pentobarbital, and the right kidney was exposed via a right flank incision, dissected free from the adrenal gland, and completely removed. Rats were maintained in metabolic cages for 24 h before the experiment in vivo to measure normal urine output and urinary levels of creatinine, protein, and HA. Metabolic and pharmacokinetic studies were performed 4 weeks after nephrectomy. Correlations of HA clearance with the clearance of either creatinine, PAH, or protein expression of rOats were examined between weeks 1 and 6 after nephrectomy. The blood urea nitrogen (BUN) was determined with the urease/indophenol method (Mizuno et al., 1997) and creatinine in serum and urine was determined by the Jaffé reaction. Measurements were performed using assay kits from Wako Pure Chemicals (Osaka, Japan). The concentration of endogenous HA in serum and urine was measured by high-performance liquid chromatography (HPLC) (Tsutsumi et al., 2002). Clearance of endogenous HA and creatinine was calculated by dividing the rate of urinary excretion by the serum concentration. The renal secretory clearance of endogenous HA was calculated by subtracting creatinine clearance multiplying the unbound fraction of HA, as the glomerular filtration rate (GFR), from renal clearance of HA. Urine protein levels were determined using the Bradford assay (Bradford, 1976).

Tissue Distribution of HA. After normal and 5/6 Nx rats were sacrificed by decapitation, their brain, heart, lungs, liver, kidneys, spleen, testes, and skeletal muscles were removed and weighed. A sample (0.5 g) of each tissue was homogenized in 5 ml of 1 M KH_2PO_4. A 50-μl aliquot of this solution was added directly to 100 μl of acetonitrile. After centrifugation at 3000*g* for 10 min, the supernatant was assayed by HPLC. The distribution of HA in each tissue is expressed as the K_p value (concentration of HA per gram of each tissue, divided by the concentration of HA in serum).

Pharmacokinetics of HA in Anesthetized Rats. Under light anesthesia with 60 mg/kg phenobarbital, normal Wistar rats (250–290 g) and 5/6 Nx rats underwent a surgical procedure in which cannulas were inserted into the femoral vein and artery using polyethylene tubing (polyethylene-50; i.d., 0.58 mm; o.d., 0.9655 mm; BD Biosciences, Parsippany, NJ) (Deguchi et al., 2003). The bile duct was also cannulated with polyethylene tubing (polyethylene-10; i.d., 0.28 mm; o.d., 0.61 mm), as was the bladder (polyethylene-8; o.d., 2.33 mm; Hibiki Co., Tokyo, Japan). Body temperature of the rats was maintained using a warming lamp. Tracer amounts of [^{14}C]HA (3 μCi/kg) or [^{3}H]PAH (2 μCi/kg) were administered with radiolabeled inulin [[^{3}H]inulin (10 μCi/kg) or [^{14}C]carboxyl-inulin (0.15 μCi/kg)] as a rapid infusion into the femoral vein. GFR was assumed to be equal to the renal clearance of inulin. After each infusion, the cannulas were flushed with a small volume of heparinized saline to ensure the complete administration of each dose and to prevent clot formation. Blood samples (200 μl) were taken from the femoral artery at a designated time. To avoid an effect on the pharmacokinetics, only four blood samples were taken from each rat. Blood was placed in graduated microcentrifuge tubes containing a drop of heparinized saline, which served as an anticoagulant. Blood samples were centrifuged (3000*g* for 10 min), and plasma was removed. Bile and urine were collected at 0 to 30, 30 to 60, 60 to 90, 90 to 120, 120 to 150, 150 to 180, and 180 to 240 min postinjection. Hionic-fluor (10 ml; PerkinElmer Life and Analytical Sciences) was added to aliquots (50 μl) of plasma, bile, and urine, followed by measurement of double-isotope radioactivity with a liquid scintillation counter. The radioactivity of an aliquot of the solution used for the injection was measured simultaneously.

Determination of the Unbound Concentration. Plasma concentrations of unbound HA were estimated by ultrafiltration as described previously (Tsutsumi et al., 1999). Free fractions of HA were calculated according to the following equation:

$$f_u = \frac{C_f}{C_t} \times 100(\%) \quad (1)$$

where f_u represents the free fraction of HA, C_f represents the free concentration of HA, and C_t represents the total concentration of HA.

Western Blot Analysis. The rat kidney plasma membrane fraction was prepared using the standard procedure (Nakajima et al., 2000). Rat kidney plasma membrane proteins (40 μg) were electrophoresed on 10% SDS-polyacrylamide gel with a 4.4% stacking gel. Separated proteins were transferred to a polyvinylidene diflouride membrane using a blotter at 15 V for 1 h. The membrane was blocked with Tris-buffered saline (137 mM NaCl and 20 mM Tris, pH 7.5) containing 0.1% Tween 20 (TBS-T) and 5% skimmed milk for 1 h at room temperature. After washing three times with TBS-T for 5 min, the membrane was incubated over night at 4°C with primary antibody specific for rOat1 (1:2000 dilution), rOat3 (1:2000 dilution), or Na^+-K^+ ATPase (1:10,000 dilution). After washing, the membrane was incubated with a horseradish peroxidase-labeled anti-rabbit IgG antibody (Amersham Biosciences UK, Ltd., Little Chalfont, Buckinghamshire, UK) diluted 1:2500 in TBS-T for 1 h at room temperature, and labeling was detected using ECL Plus (Amersham Biosciences UK, Ltd.).

Data and Statistical Analysis. Plasma concentration profiles were analyzed by fitting the following biexponential equation using the nonlinear least-squares method (MULTI) (Yamaoka et al., 1981):

$$C_p = A \times \exp^{(-\alpha \times t)} + B \times \exp^{(-\beta \times t)} \quad (2)$$

Pharmacokinetic parameters were calculated using the following equations:

$$AUC_{0\to\infty} = \frac{A}{\alpha} + \frac{B}{\beta} \quad (3)$$

$$CL_{tot} = \frac{Dose}{AUC_{0\to\infty}} \quad (4)$$

$$t_{1/2\beta} = \frac{0.693}{\beta} \quad (5)$$

$$CL_{renal} = CL_{tot} \times f_{urine} \quad (6)$$

$$CL_{biliary} = CL_{tot} \times f_{bile} \quad (7)$$

where $AUC_{0\to\infty}$, CL_{tot}, $t_{1/2\beta}$, CL_{renal}, f_{urine}, CL_{bile}, and f_{bile}, represent the AUC from zero to infinity, total body clearance, β-phase half-life, renal clearance, fraction of test compound recovered in the urine, biliary clearance, and fraction of test compound recovered in the bile, respectively.

Unless otherwise indicated, all data represent the mean ± S.E., and *n* refers to the number of animals used in each experiment. An unpaired, two-tailed Student's *t* test was used to determine the significance of differences between means of two groups. Fitting was performed using the nonlinear least-squares method with the MULTI program and the Damping Gauss Newton Method algorithm (Yamaoka et al., 1981).

Results

Renal Function in Normal and 5/6 Nx Rats. Four weeks after nephrectomy, 5/6 Nx rats exhibited significant increases in urine volume, BUN, serum creatinine, proteinuria, and serum concentration of endogenous HA (Table 1). In addition, there was a decrease in body weight and creatinine clearance, indicating that renal function was significantly impaired in 5/6 Nx rats.

Pharmacokinetics of HA in 5/6 Nx Rats. Table 2 shows the tissue distribution of endogenous HA in control and 5/6 Nx rats. These results indicate that the highest concentration of HA occurred in the kidney. The HA tissue-to-serum concentration ratio (K_p) was markedly reduced in 5/6 Nx rat kidneys, compared with the normal rat kidneys. In contrast, the K_p value of the brain was significantly increased in 5/6 Nx rats compared with control rats.

To roughly delineate the major route for elimination of HA from plasma, we examined urinary and biliary excretion in normal and 5/6 Nx rats (Fig. 1; Table 3). Most of the HA was excreted in an intact form (data not shown), and the main route was via the urine (Fig. 1B). The plasma clearance of HA was significantly decreased in 5/6 Nx rats. The biological half-life of HA was longer in 5/6 Nx rats (156 min) than in the control rats (22 min). These values seem to reflect plasma and renal clearance, suggesting that plasma clearance of HA was reduced by impairment of renal function. The unbound fraction of HA was increased in 5/6 Nx rats compared with control rats (Table 3), indicating that plasma protein binding of HA was inhibited by other strongly protein-bound uremic retention compounds, such as 3-carboxy-4-methyl-5-propyl-2-furanpropanoic acid and indoxyl sulfate. In normal rats, the renal clearance of unbound HA was about 16 times greater than the GFR, which suggests that active tubular secretion is involved in the urinary excretion of HA. The excretion ratio of 5/6 Nx rats was 50% of that of control rats, an indication that the contribution of secretion to the renal elimination of HA was reduced in 5/6 Nx rats.

TABLE 1

Physiological parameters of normal and 5/6 Nx rats 4 weeks after nephrectomy

Each value represents the mean ± S.E. of 15 to 20 experiments.

Parameter	Normal Rats	5/6 Nx Rats
Body weight (g)	339 ± 5	307 ± 6*
Urine volume (ml/day)	8.89 ± 1.04	19.6 ± 0.9*
BUN (mg/ml)	15.4 ± 0.5	43.1 ± 1.3*
Serum creatinine (mg/dl)	0.758 ± 0.024	1.89 ± 0.10*
Creatinine clearance (ml/min/kg)	2.83 ± 0.09	1.58 ± 0.06*
Proteinuria (μg/min/kg)	18.3 ± 2.2	152 ± 31*
Endogenous serum HA (μM)	12.3 ± 2.4	135 ± 12*

* $p < 0.01$, significantly different from the corresponding parameter in normal rats.

Dose-Dependent Pharmacokinetics of HA in Normal Rats. We examined the dose dependence of pharmacokinetic parameters after iv. administration of HA (Fig. 2A). Plasma clearance decreased as the dosage increased from 0.1 to 5 mg/kg (Table 4), indicating that renal tubular secretion is the main route for elimination of HA. In normal rats, renal clearance of HA was comparable with that of PAH (Table 4), which suggests that the excretion rate of HA (like that of PAH) was determined by the renal plasma flow rate.

Correlation between Renal Clearance of Endogenous HA and Creatinine Clearance, PAH Clearance, and Expression Levels of Renal Organic Anion Transporters. To evaluate the renal clearance of endogenous HA corrected by the unbound fraction as a clinical marker, we examined the linear regression of the renal clearance of unbound HA against creatinine clearance (Fig. 3A) and PAH clearance corrected by its unbound fraction (Fig. 3B). In normal and 5/6 Nx rats, the renal clearance of unbound HA correlated more closely with clearance of unbound PAH ($r = 0.846$; $p < 0.01$) than with the clearance of creatinine ($r = 0.571$; $p < 0.01$).

We used Western blotting to assess the expression levels of renal rOats. We observed primary bands for rOat1, rOat3, and Na^+-K^+ ATPase with sizes of 62, 71, and 125 kDa, respectively (Fig. 4A). Compared with normal rats, the kidneys of 5/6 Nx rats had markedly decreased protein expression levels of rOat1 (42.0% of normal) and rOat3 (49.3% of normal) (Fig. 4B), whereas there was no significant difference in expression of Na^+-K^+ ATPase between the normal and 5/6 Nx rats (Fig. 4A). Figure 4C shows the correlation between the renal secretory clearance of endogenous HA and expression levels of rOats in 5/6 Nx rats. The renal secretory clearance of HA significantly correlated with the levels of rOat1 ($r = 0.786$; $p < 0.01$) and rOat3 ($r = 0.653$; $p < 0.01$).

Discussion

Endogenous HA was mainly localized in the kidney in control and 5/6 Nx rats (Table 2), and the renal concentration of HA in 5/6 Nx rats was approximately 3 times greater than that of normal rats. It has been suggested that the uptake mechanism of HA plays a key role in the induction of HA nephrotoxicity (Satoh et al., 2003). Interestingly, the K_p value in the brain was significantly greater for 5/6 Nx rats than for control rats. HA is markedly elevated in the serum and cerebrospinal fluid of uremic patients (Porter et al.,

TABLE 2

Tissue distribution of endogenous HA in normal and 5/6 Nx rats 4 weeks after nephrectomy

Endogenous HA was measured in various tissues of normal and 5/6 Nx rats by HPLC. Distribution of HA in each tissue is expressed as K_p, i.e., the concentration of HA per gram of each tissue divided by concentration of HA in serum (normal rats, 12.3 ± 1.0 μM; 5/6 Nx rats, 132 ± 9 μM). Each value represents the mean ± S.E. of three experiments.

	Normal Rats		5/6 Nx Rats	
	Concentration	K_p	Concentration	K_p
	nmol/mg tissue	*ml/g tissue*	*nmol/mg tissue*	*ml/g tissue*
Brain	1.62 ± 0.17	0.132 ± 0.015	72.8 ± 9.1	0.549 ± 0.044*
Heart	6.28 ± 0.23	0.515 ± 0.028	64.9 ± 6.1	0.492 ± 0.025
Lung	12.3 ± 3.9	0.987 ± 0.267	142 ± 10	1.08 ± 0.02
Liver	18.2 ± 2.7	1.51 ± 0.29	180 ± 14	1.36 ± 0.04
Kidney	258 ± 19	21.1 ± 1.4	723 ± 14	5.55 ± 0.44*
Spleen	7.72 ± 2.52	0.607 ± 0.183	84.6 ± 3.1	0.648 ± 0.045
Testis	6.60 ± 1.85	0.519 ± 0.119	64.5 ± 4.8	0.471 ± 0.053
Skeletal muscle	2.47 ± 0.56	0.197 ± 0.036	24.1 ± 4.1	0.180 ± 0.018

* $p < 0.01$, significantly different from the corresponding parameter in normal rats.

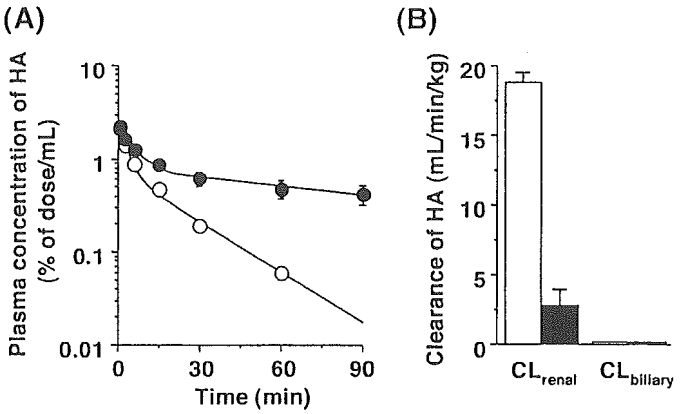

Fig. 1. Disposition profiles after i.v. administration of [^{14}C]HA in normal and 5/6 Nx rats 4 weeks after nephrectomy. A, HA was administered at a dose of 0.1 mg/kg by rapid infusion into the femoral vein in normal (○) and 5/6 Nx rats (●). B, bile and urine (normal rats, □; 5/6 Nx rats, ■) were collected at 180 min postinjection. See *Materials and Methods* for experimental details. Each point represents the mean ± S.E. of four or five experiments.

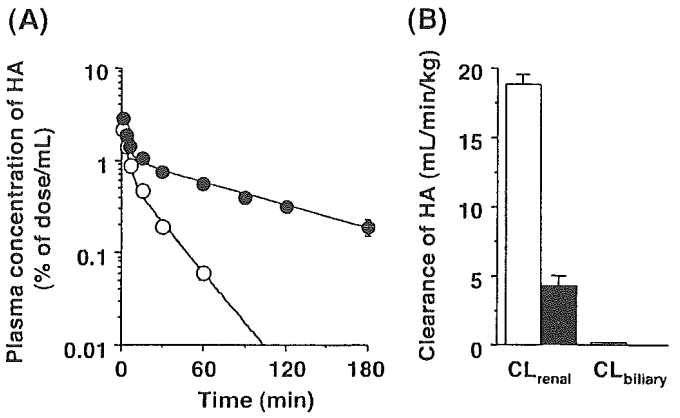

Fig. 2. Dose-dependent pharmacokinetics of HA after i.v. administration. A, HA was administered at a dose of 0.1 mg/kg (○) or 5 mg/kg (●) by rapid infusion into the femoral vein in normal rats. B, bile and urine (0.1 mg/kg, □; 5 mg/kg, ■) were collected at 180 min postinjection. See *Materials and Methods* for experimental details. Each point represents the mean ± S.E. of four experiments.

TABLE 3

Pharmacokinetic parameters of [^{14}C]HA after i.v. administration to normal and 5/6 Nx rats 4 weeks after nephrectomy (0.1 mg/kg)

GFR was assumed to be equal to the renal clearance of inulin in normal or 5/6 Nx rats. Excretion ratio was calculated by dividing the renal clearance by the unbound fraction and GFR. Each value represents the mean ± S.E. of four or five experiments.

Parameter	Normal Rats	5/6 Nx Rats
AUC (% of dose/ml · min)	25.1 ± 1.1	165 ± 49*
$t_{1/2\beta}$ (min)	21.9 ± 1.3	156 ± 64*
$V_{d,ss}$ (ml/kg)	440 ± 22	401 ± 65
CL_{tot} (ml/min/kg)	19.3 ± 0.7	3.55 ± 1.57**
CL_{renal} (mL/min/kg)	18.1 ± 0.7	2.68 ± 1.19**
$CL_{biliary}$ (ml/min/kg)	0.092 ± 0.010	0.10 ± 0.01
GFR (ml/min/kg)	2.43 ± 0.18	0.59 ± 0.13**
f_u (%)	47.4 ± 1.7	60.3 ± 0.8**
Excretion ratio	15.7	7.56

* $p < 0.05$, ** $p < 0.01$, significantly different from the corresponding parameter in normal rats.

TABLE 4

Pharmacokinetic parameters of PAH and dose-dependent pharmacokinetics of HA after i.v. administration to normal rats

GFR was assumed to be equal to the renal clearance of inulin in normal rats (2.43 ± 0.18 ml/min/kg, $n = 4$). Excretion ratio was calculated by dividing the renal clearance by the unbound fraction and GFR. Each value represents the mean ± S.E. of four experiments.

Parameter	PAH (0.1 mg/kg)	HA	
		0.1 mg/kg	5 mg/kg
AUC (% of dose/ml · min)	24.3 ± 1.5	25.1 ± 1.1	115 ± 15*
$t_{1/2\beta}$ (min)	24.5 ± 2.2	21.9 ± 1.3	73.9 ± 4.4*
$V_{d,ss}$ (ml/kg)	612 ± 37	440 ± 22	433 ± 41
CL_{tot} (ml/min/kg)	21.8 ± 1.5	19.3 ± 0.7	4.57 ± 0.68*
CL_{renal} (ml/min/kg)	20.4 ± 1.5	18.1 ± 0.7	4.24 ± 0.64*
f_u (%)	91.0 ± 1.6	47.4 ± 1.7	46.0 ± 1.1
Excretion ratio	9.22	15.7	3.80

* $p < 0.01$, significantly different from the corresponding parameter of 0.1 mg/kg HA.

1975). In addition, the serum concentration of HA in hemodialysis patients correlates positively with neurophysiological indices (Schoots et al., 1989), suggesting that HA is related to neurological symptoms in uremia. Likewise, a relationship was observed in patients between the increasing severity of abnormalities attributable to the uremic state and higher plasma concentrations of 3-carboxy-4-methyl-5-propyl-2-furanpropanoic acid (Costigan et al., 1996). Evidence obtained by Ohtsuki et al. (2002) suggests that uremic toxins (e.g., indoxyl sulfate and HA) inhibit rOat3-mediated brain-to-blood transport in uremic patients, leading to accumulation of neurotransmitter metabolites and drugs in the brain (Ohtsuki et al., 2002). These findings highlight the importance of carrier-mediated transport of uremic toxins such as HA across the blood-brain barrier and the mechanism of neurological symptoms of uremic syndrome in CRF patients.

In the present study, we examined the distribution of the

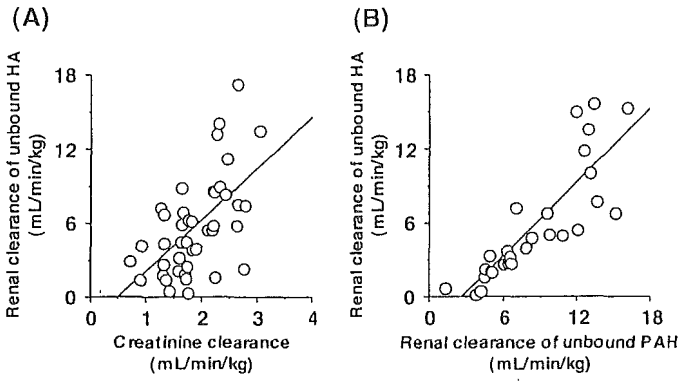

Fig. 3. Linear regression of endogenous HA clearance against endogenous creatinine clearance (A) and [^{3}H]PAH clearance (B) in normal and 5/6 Nx rats. The serum and urinary concentration of HA were measured by HPLC, and endogenous HA clearance was calculated.

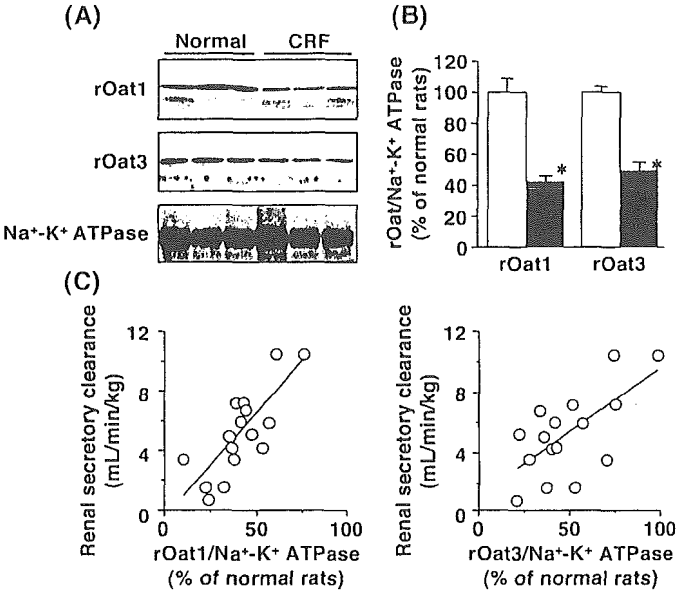

Fig. 4. Protein expression of rOat1 and rOat3 in normal and 5/6 Nx rats and correlation between rOat expression and the renal secretory clearance of endogenous HA. The protein expression levels of rOat1, rOat3, and Na^+-K^+ ATPase were determined by Western blotting as outlined under *Materials and Methods*. A, image shows a blot of the crude plasma membranes isolated from normal or 5/6 Nx rats 4 weeks after nephrectomy. We observed a 62-kDa band for rOat1, a 71-kDa band for rOat3, and a 125-kDa band for Na^+-K^+ ATPase. B, average mass of each protein band is expressed as units of the densitometry ratio of rOats to Na^+-K^+ ATPase for normal (open column) and 5/6 Nx rats (closed column). The values for normal rats were arbitrarily defined as 100%. Each column represents the mean ± S.E. (7–10). *, $p < 0.01$, significantly different from normal rats. C, image shows the correlation between the expression levels of renal rOats and renal secretory clearance of endogenous HA in 5/6 Nx rats.

uremic toxin HA in normal and 5/6 Nx rats after i.v. administration of HA. The total clearance of HA was equal to the renal clearance, and nearly all excreted HA was eliminated via the kidney (Table 2) in a largely unchanged form. Additionally, the plasma and renal clearance of HA was significantly decreased in 5/6 Nx rats (Fig. 1), indicating that HA is mainly excreted via the kidney. In normal rats, the renal clearance of unbound HA was about 16 times greater than the GFR, which suggests that active tubular secretion is involved in the urinary excretion of HA. Furthermore, our observations indicated that the plasma clearance of HA was dose-dependent (Fig. 2; Table 4). HA significantly inhibited PAH transport in the kidney (Boumendil-Podevin et al., 1975), suggesting that both compounds are transported by the organic anion transport system. Recently, we demonstrated that rOat1 and human OAT1 (hOAT1) play an important role in renal uptake of HA (Deguchi et al., 2004). Together, these findings indicate that organic anion transporters play an important role in renal transport of HA and that functional failure of the system responsible for excretion of HA causes accumulation of HA in blood. The renal clearance of HA has been reported to be 590 ml/min in healthy people (Ilic et al., 2000), suggesting that HA is also rapidly and efficiently cleared by the kidney in rats. In the normal rats of the present study, the renal clearance of HA was comparable with that of PAH (Table 4), indicating that the excretion rate of HA (like that of PAH) is dependent on the renal plasma flow rate.

Residual nephrons make a significant contribution to the removal of uremic waste products in patients on chronic dialysis treatment (van Olden et al., 1998). HA is one of the most abundant waste products in uremic serum, accumulating to concentrations as high as 2.5 mM (Vanholder et al., 2003), and HA suppresses PAH transport by the kidney (Boumendil-Podevin et al., 1975). These findings indicate that accumulation of uremic toxins, including HA inhibit both their own renal elimination and that of other organic anions by inhibiting transport via rOats/hOATs (Deguchi et al., 2004). Therefore, the inhibition of rOats by HA and other uremic toxins accumulated in serum may be partly involved in the decrease of HA clearance in 5/6 Nx rats (Table 3). These observations also suggest that serum HA is a useful indicator of interactions between uremic toxins and drugs in patients with uremia. In addition, plasma and urine specimens from healthy subjects contain small amounts of uremic toxins (Sakai et al., 1996), allowing quantification of renal clearance in vivo and prediction of renal anion secretion. In the 5/6 Nx rats of the present study, the renal clearance of unbound HA correlated more closely with the clearance of unbound PAH than with the clearance of creatinine (Fig. 3), which implies that renal clearance of endogenous HA reflects the renal secretion of organic anions. It is known that a small fraction of creatinine is cleared through active tubular secretion, partially by human organic cation transporter 2 (hOCT2; SLC22A)-mediated transport (Urakami et al., 2004). In CRF, the urinary excretion of cationic substrates is reduced, partly because of the reduced expression of OCT2 (Ji et al., 2002), which suggests that both renal secretion of creatinine and glomerular filtration may be attenuated. Although it is difficult to estimate the contributions of GFR and secretion in CRF, the present results suggest that the renal clearance of HA would not reflect glomerular filtration and OCTs-mediated secretion.

In renal tubules, membrane transport systems mediate the tubular secretion of endogenous and exogenous organic anions, including various drugs, toxins, and endogenous metabolites. rOat1 (*Slc22a6*), a typical substrate of which is PAH, is expressed predominantly in the kidney and is localized on the basolateral membrane of the middle proximal tubules (S2) (Kusuhara and Sugiyama, 2002; Miyazaki et al., 2004). rOat1 has broad substrate specificity and transports a variety of organic anions. Other isoforms in rodents, referred to as Oat2 (*Slc22a7*), Oat3 (*Slc22a8*), and Oat5 (*Slc22a19*), are

expressed in the kidney (Kusuhara and Sugiyama, 2002; Youngblood and Sweet, 2004). Immunolocalization studies have revealed that Oat2 is apical in rat kidney, but basolateral in human kidney (Enomoto et al., 2002; Kojima et al., 2002). Additionally, the localization of Oat5 in the kidney has not been identified yet and so the role of Oat2 and Oat5 in the renal transport of organic anions is unclear. In human kidney, the renal brush-border membrane possesses an influx/efflux transport system for organic anions, such as hOAT4 (*SLC22A11*), and it has been suggested that hOAT4 is partly involved in the apical efflux of uremic toxins in human proximal tubules (Enomoto et al., 2003). rOat3 expressed in the kidney is located on the basolateral membrane of all segments (S1, S2, and S3) of the proximal tubules (Kusuhara and Sugiyama, 2002; Miyazaki et al., 2004). Functional characterization shows that substrates of rOat3 include organic anions and the organic cation cimetidine (Kusuhara and Sugiyama, 2002; Hasegawa et al., 2003). The contribution of rOat1 and rOat3 to renal uptake of organic anions has been evaluated with kidney slices and the results suggest that rOat1 is the primary mediator of the renal uptake of small hydrophilic molecules, whereas rOat3 mediates renal uptake of more bulky organic anions (Hasegawa et al., 2003). It has also been reported that uptake of taurocholate, estrone sulfate and PAH by kidney slices is markedly reduced in mOat3 knockout mice (Sweet et al., 2002). hOAT1 and hOAT3 are predominantly expressed in the kidney and are coexpressed on the basolateral membrane in some parts of the proximal tubules (Hosoyamada et al., 1999; Cha et al., 2001; Motohashi et al., 2002). Given the results of transport studies in rats and mice, it is thought that hOAT1 and hOAT3 play a predominant role in the transport of organic anions across the basolateral membrane of human proximal tubules.

In patients with renal failure, pathophysiological changes may affect the activity of transporters. As mentioned above, uremic toxins, especially HA, seem to inhibit OAT1- and OAT3-mediated transport in vivo in cases of CRF (Deguchi et al., 2004), leading to an acceleration of the accumulation of uremic toxins in serum. On the other hand, the expression levels of some transporters are changed in 5/6 Nx rats and patients with renal disease (Laouari et al., 2001; Ji et al., 2002; Sakurai et al., 2004), which suggests that expression levels of drug transporters are related to changes in renal anion secretion. The present Western blot analysis demonstrated that the protein expression levels of rOat1 and rOat3 were markedly decreased in the kidneys of 5/6 Nx rats compared with normal rats (Fig. 4B), reflecting the fact that 5/6 Nx rats have a decreased K_p value of endogenous HA in the kidneys (Table 2) and a decreased excretion ratio of HA (Table 3). This result agrees with previous work using cDNA array and quantitative reverse transcription-polymerase chain reaction analysis (Aoyama et al., 2003). Furthermore, the renal secretory clearance of endogenous HA correlated significantly with the levels of rOat1 and rOat3 (Fig. 4C). This suggests that the changes in expression levels of rOat1 and rOat3 may affect the secretion of renal anions such as HA in uremia. The present results indicate that HA is suitable as a reference compound for estimation of renal clearance of organic anions and protein expression of OATs. Such information could be used to prevent excessive accumulation of drugs in the body before treatment. In the previous report, rOat1 mainly accounted for HA uptake in the kidney (Deguchi et al., 2004). However, protein expression of rOat3 correlated with renal clearance of HA. There are two possibilities that may account for this. First, HA is partly taken up by rOat3. Our kinetic experiments suggested that rOat1 accounted for about 70% of the renal uptake of HA, and the remaining fraction was accounted for by a pravastatin- or benzylpenicillin-sensitive transporter, which may be rOat3 (Deguchi et al., 2004). Second, rOat1 and rOat3 are coregulated in 5/6 Nx rats. Previous determinations of chromosomal locations noted that OAT1 and OAT3 genes are tightly linked in the mouse and human genomes (Eraly et al., 2003), which suggests that the pairing might exist to facilitate the coregulation of their genes. Protein expression of rOat3 could therefore be correlated indirectly with the renal clearance of HA. On the other hand, it has been reported that normal expression levels of rOat1 and rOat3 protein are maintained in rats 2 weeks after 5/6 nephrectomy (Ji et al., 2002). However, in the present study, 5/6 Nx rats were used for experiments more than 4 weeks after surgery. Thus, there may be a progressive reduction of the renal expression of rOat1 and rOat3 after 5/6 nephrectomy.

In conclusion, the results of the present experiments in vivo with 5/6 Nx rats indicate that the primary route for elimination of HA from the plasma is via the kidney by active tubular secretion, and that renal clearance of endogenous HA is a useful indicator of the changes in renal secretion that accompany reduction of OATs protein expression in CRF.

References

Aoyama I, Enomoto A, and Niwa T (2003) Effects of oral adsorbent on gene expression profile in uremic rat kidney: cDNA array analysis. *Am J Kidney Dis* **41**:S8–S14.

Boumendil-Podevin EF, Podevin RA, and Richet G (1975) Uricosuric agents in uremic sera. Identification of indoxyl sulfate and hippuric acid. *J Clin Investig* **55**:1142–1152.

Bradford MM (1976) A rapid and sensitive method for the quantitation of microgram quantities of protein utilizing the principle of protein-dye binding. *Anal Biochem* **72**:248–254.

Cha SH, Sekine T, Fukushima JI, Kanai Y, Kobayashi Y, Goya T, and Endou H (2001) Identification and characterization of human organic anion transporter 3 expressing predominantly in the kidney. *Mol Pharmacol* **59**:1277–1286.

Costigan MG, Callaghan CA, and Lindup WE (1996) Hypothesis: is accumulation of a furan dicarboxylic acid (3-carboxy-4-methyl-5-propyl-2-furanpropanoic acid) related to the neurological abnormalities in patients with renal failure? *Nephron* **73**:169–173.

Deguchi T, Kusuhara H, Takadate A, Endou H, Otagiri M, and Sugiyama Y (2004) Characterization of uremic toxin transport by organic anion transporters in the kidney. *Kidney Int* **65**:162–174.

Deguchi T, Nakamura M, Tsutsumi Y, Suenaga A, and Otagiri M (2003) Pharmacokinetics and tissue distribution of uraemic indoxyl sulphate in rats. *Biopharm Drug Dispos* **24**:345–355.

Dzurik R, Spustova V, Krivosikova Z, and Gazdikova K (2001) Hippurate participates in the correction of metabolic acidosis. *Kidney Int Suppl* **78**:S278–S281.

Enomoto A, Takeda M, Shimoda M, Narikawa S, Kobayashi Y, Yamamoto T, Sekine T, Cha SH, Niwa T, and Endou H (2002) Interaction of human organic anion transporters 2 and 4 with organic anion transport inhibitors. *J Pharmacol Exp Ther* **301**:797–802.

Enomoto A, Takeda M, Taki K, Takayama F, Noshiro R, Niwa T, and Endou H (2003) Interactions of human organic anion as well as cation transporters with indoxyl sulfate. *Eur J Pharmacol* **466**:13–20.

Eraly SA, Hamilton BA, and Nigam SK (2003) Organic anion and cation transporters occur in pairs of similar and similarly expressed genes. *Biochem Biophys Res Commun* **300**:333–342.

Hasegawa M, Kusuhara H, Endou H, and Sugiyama Y (2003) Contribution of organic anion transporters to the renal uptake of anionic compounds and nucleoside derivatives in rat. *J Pharmacol Exp Ther* **305**:1087–1097.

Hosoyamada M, Sekine T, Kanai Y, and Endou H (1999) Molecular cloning and functional expression of a multispecific organic anion transporter from human kidney. *Am J Physiol* **276**:F122–F128.

Ilic S, Rajic M, Vlajkovic M, Bogicevic M, and Stefanovic V (2000) The predictive value of 131I-hippurate clearance in the prognosis of acute renal failure. *Ren Fail* **22**:581–589.

Ji L, Masuda S, Saito H, and Inui K (2002) Down-regulation of rat organic cation transporter rOCT2 by 5/6 nephrectomy. *Kidney Int* **62**:514–524.

Kojima R, Sekine T, Kawachi M, Cha SH, Suzuki Y, and Endou H (2002) Immunolocalization of multispecific organic anion transporters, OAT1, OAT2 and OAT3, in rat kidney. *J Am Soc Nephrol* **13**:848–857.

Kusuhara H and Sugiyama Y (2002) Role of transporters in the tissue-selective distribution and elimination of drugs: transporters in the liver, small intestine, brain and kidney. *J Control Release* 78:43–54.

Laouari D, Yang R, Veau C, Blanke I, and Friedlander G (2001) Two apical multidrug transporters, P-gp and MRP2, are differently altered in chronic renal failure. *Am J Physiol* 280:F636–F645.

Miyazaki H, Sekine T, and Endou H (2004) The multispecific organic anion transporter family: properties and pharmacological significance. *Trends Pharmacol Sci* 25:654–662.

Mizuno S, Yue BF, Okamoto M, Horikawa Y, and Kurosawa T (1997) Diffuse glomerulosclerosis without tubular injury does not directly manifest renal dysfunction in nephrotic mice (ICGN strain). *Exp Nephrol* 5:498–507.

Motohashi H, Sakurai Y, Saito H, Masuda S, Urakami Y, Goto M, Fukatsu A, Ogawa O, and Inui K (2002) Gene expression levels and immunolocalization of organic ion transporters in the human kidney. *J Am Soc Nephrol* 13:866–874.

Nakajima N, Sekine T, Cha SH, Tojo A, Hosoyamada M, Kanai Y, Yan K, Awa S, and Endou H (2000) Developmental changes in multispecific organic anion transporter 1 expression in the rat kidney. *Kidney Int* 57:1608–1616.

Niwa T (1996) Organic acids and the uremic syndrome: protein metabolite hypothesis in the progression of chronic renal failure. *Semin Nephrol* 16:167–182.

Ohtsuki S, Asaba H, Takanaga H, Deguchi T, Hosoya K, Otagiri M, and Terasaki T (2002) Role of blood-brain barrier organic anion transporter 3 (OAT3) in the efflux of indoxyl sulfate, a uremic toxin: its involvement in neurotransmitter metabolite clearance from the brain. *J Neurochem* 83:57–66.

Porter RD, Cathcart-Rake WF, Wan SH, Whittier FC, and Grantham JJ (1975) Secretory activity and aryl acid content of serum, urine and cerebrospinal fluid in normal and uremic man. *J Lab Clin Med* 85:723–731.

Sakai T, Maruyama T, Imamura H, Shimada H, and Otagiri M (1996) Mechanism of stereoselective serum binding of ketoprofen after hemodialysis. *J Pharmacol Exp Ther* 278:786–792.

Sakai T, Takadate A, and Otagiri M (1995) Characterization of binding site of uremic toxins on human serum albumin. *Biol Pharm Bull* 18:1755–1761.

Sakurai Y, Motohashi H, Ueo H, Masuda S, Saito H, Okuda M, Mori N, Matsuura M, Doi T, Fukatsu A, et al. (2004) Expression levels of renal organic anion transporters (OATs) and their correlation with anionic drug excretion in patients with renal diseases. *Pharm Res* 21:61–67.

Satoh M, Hayashi H, Watanabe M, Ueda K, Yamato H, Yoshioka T, and Motojima M (2003) Uremic toxins overload accelerates renal damage in a rat model of chronic renal failure. *Nephron Exp Nephrol* 95:e111–e118.

Schoots AC, De Vries PM, Thiemann R, Hazejager WA, Visser SL, and Oe PL (1989) Biochemical and neurophysiological parameters in hemodialyzed patients with chronic renal failure. *Clin Chim Acta* 185:91–107.

Spustova V, Cernay P, and Golier I (1989) Inhibition of glucose utilization in uremia by hippurate: liquid chromatographic isolation and mass spectrometric and nuclear magnetic resonance spectroscopic identification. *J Chromatogr* 490:186–192.

Spustova V, Dzurik R, and Gerykova M (1987) Hippurate participation in the inhibition of glucose utilization in renal failure. *Czech Med* 10:79–89.

Sweet DH, Miller DS, Pritchard JB, Fujiwara Y, Beier DR, and Nigam SK (2002) Impaired organic anion transport in kidney and choroid plexus of organic anion transporter 3 (Oat3 (Slc22a8)) knockout mice. *J Biol Chem* 277:26934–26943.

Tsutsumi Y, Deguchi T, Takano M, Takadate A, Lindup WE, and Otagiri M (2002) Renal disposition of a furan dicarboxylic acid and other uremic toxins in the rat. *J Pharmacol Exp Ther* 303:880–887.

Tsutsumi Y, Maruyama T, Takadate A, Goto M, Matsunaga H, and Otagiri M (1999) Interaction between two dicarboxylate endogenous substances, bilirubin and an uremic toxin, 3-carboxy-4-methyl-5-propyl-2-furanpropanoic acid, on human serum albumin. *Pharm Res* 16:916–923.

Urakami Y, Kimura N, Okuda M, and Inui K (2004) Creatinine transport by basolateral organic cation transporter hOCT2 in the human kidney. *Pharm Res* 21: 976–981.

Vanholder R, De Smet R, Glorieux G, Argiles A, Baurmeister U, Brunet P, Clark W, Cohen G, De Deyn PP, Deppisch R, et al. (2003) Review on uremic toxins: classification, concentration and interindividual variability. *Kidney Int* 63:1934–1943.

van Olden RW, van Acker BA, Koomen GC, Krediet RT, and Arisz L (1998) Contribution of tubular anion and cation secretion to residual renal function in chronic dialysis patients. *Clin Nephrol* 49:167–172.

Yamaoka K, Tanigawara Y, Nakagawa T, and Uno T (1981) A pharmacokinetic analysis program (multi) for microcomputer. *J Pharmacobio-Dyn* 4:879–885.

Youngblood GL and Sweet DH (2004) Identification and functional assessment of the novel murine organic anion transporter Oat5 (Slc22a19) expressed in kidney. *Am J Physiol* 287:F236–F244.

Address correspondence to: Professor Masaki Otagiri, Department of Biopharmaceutics, Graduate School of Pharmaceutical Sciences, Kumamoto University, 5-1 Oe-honmachi, Kumamoto 862-0973, Japan. E-mail: otagirim@gpo.kumamoto-u.ac.jp

Journal of Neurochemistry, 2006, **96**, 1051–1059 doi:10.1111/j.1471-4159.2005.03550.x

Involvement of organic anion transporters in the efflux of uremic toxins across the blood–brain barrier

Tsuneo Deguchi,* Kouya Isozaki,* Kouno Yousuke,* Tetsuya Terasaki† and Masaki Otagiri*

**Department of Biopharmaceutics, Graduate School of Pharmaceutical Sciences, Kumamoto University, Kumamoto, Japan*
†Department of Molecular Biopharmacy and Genetics, Graduate School of Pharmaceutical Sciences and New Industry Creation Hatchery Center, Tohoku University, Sendai, and Core Research for Evolutional Science and Technology and Solution Oriented Research for Science and Technology of the Japan Science and Technology Agency, Japan

Abstract

Renal failure causes multiple physiological changes involving CNS dysfunction. In cases of uremia, there is close correlation between plasma levels of uremic toxins [e.g. 3-carboxy-4-methyl-5-propyl-2-furanpropionate (CMPF), hippurate (HA) and indoleacetate (IA)] and the degree of uremic encephalopathy, suggesting that uremic toxins are involved in uremic encephalopathy. In order to evaluate the relevance of uremic toxins to CNS dysfunction, we investigated directional transport of uremic toxins across the blood–brain barrier (BBB) using *in vivo* integration plot analysis and the brain efflux index method. We observed saturable efflux transport of [^{3}H]CMPF, [^{14}C]HA and [^{3}H]IA, which was inhibited by probenecid. For all uremic toxins evaluated, apparent efflux clearance across the BBB was greater than apparent influx clearance, suggesting that these toxins are predominantly transported from the brain to blood across the BBB. Saturable efflux transport of [^{3}H]CMPF, [^{14}C]HA and [^{3}H]IA was completely inhibited by benzylpenicillin, which is a substrate of rat organic anion transporter 3 (rOat3). Taurocholate and digoxin, which are common substrates of rat organic anion transporting polypeptide (rOatp), partially inhibited the efflux of [^{3}H]CMPF. Transport experiments using a *Xenopus laevis* oocyte expression system revealed that CMPF, HA and IA are substrates of rOat3, and that CMPF (but not HA or IA) is a substrate of rOap2. These results suggest that rOat3 mediates brain-to-blood transport of uremic toxins, and that rOatp2 is involved in efflux of CMPF. Thus, conditions typical of uremia can cause inhibition of brain-to-blood transport involving rOat3 and/or rOatp2, leading to accumulation of endogenous metabolites and drugs in the brain.

Keywords: blood–brain barrier, efflux transport, organic anion transporter, uremic encephalopathy, uremic toxin.
J. Neurochem. (2006) **96**, 1051–1059.

Renal insufficiency leading to uremia affects almost all bodily functions, but brain physiology appears to be particularly vulnerable to uremic toxicity (Moe and Sprague 1994). Renal failure results in accumulation of numerous organic substances that may act as uremic neurotoxins, but no single metabolite has been identified as the sole cause of uremia (Brouns and De Deyn 2004). Some of the manifestations of the resulting uremic encephalopathy, including cognitive and attentional impairments, lethargy, convulsions and coma, can be partially improved by dialysis and correction of malnutrition (Smogorzewski 2001). It has long been thought that uremic retention solutes may play a significant role in uremic pathophysiology.

High levels of 3-carboxy-4-methyl-5-propyl-2-furanpropionate (CMPF), hippurate (HA) and indoleacetate (IA) have been found in serum, CSF and brain tissue of uremic patients (Muting 1965; Costigan *et al.* 1996; Niwa 1996; Tsutsumi *et al.* 2002). One study has shown a positive correlation between neurophysiological indices of patients on hemodialysis and their serum concentration of HA (Schoots *et al.* 1989). Similarly, another study has shown a relationship between higher plasma concentrations of CMPF in patients on hemodialysis and increasing severity of abnormalities

Received June 6, 2005; revised manuscript received September 12, 2005; accepted September 23, 2005.

Address correspondence and reprint requests to Professor Masaki Otagiri, PhD, Department of Biopharmaceutics, Graduate School of Pharmaceutical Sciences, Kumamoto University, 5–1 Oe-honmachi, Kumamoto 862–0973, Japan. E-mail: otagirim@gpo.kumamoto-u.ac.jp

Abbreviations used: BBB, blood–brain barrier; BEI, brain efflux index; CMPF, 3-carboxy-4-methyl-5-propyl-2-furanpropanoic acid; HA, hippurate; IA, indoleacetate; IS, indoxyl sulfate; PAH, *p*-aminohippuric acid; PCG, benzylpenicillin; rOat3, rat organic anion transporter 3; rOatp, rat organic anion transporting polypeptide.

attributable to the uremic state (Costigan *et al.* 1996). It has been postulated that CMPF, HA and IA contribute to the epileptic and cognitive symptoms that accompany uremic encephalopathy. However, despite the importance of understanding how uremic toxins accumulate in the brain, there have been few direct studies of their transport in the brain.

The blood–brain barrier (BBB) consists of complex tight junctions of brain capillary endothelial cells, which express xenobiotic transporters (Pardridge 1999; Kusuhara and Sugiyama 2001a,b; Loscher and Potschka 2005). These transporters include members of the organic anion transporter family, the organic anion transporting polypeptide family and the ATP-binding cassette transporter family. Evidence suggests that these transporters facilitate elimination of xenobiotics and endogenous compounds from the CNS across the BBB. The concentrations of CMPF, HA and IA in CSF and brain tissue are several times lower than their concentrations in serum (Muting 1965; Porter *et al.* 1975; Tsutsumi *et al.* 2002). This disparity in distribution of CMPF, HA and IA may be due to brain-to-blood transport of uremic toxins at the BBB.

Recent reports show that rat organic anion transporter (rOat3: Slc22a8), which is localized at the rat BBB (Kikuchi *et al.* 2003; Mori *et al.* 2003), is a probenecid-sensitive transporter that mediates efflux of 6-mercaptopurine (Mori *et al.* 2004), homovanillic acid (Mori *et al.* 2003), *p*-aminohippuric acid (PAH) and benzylpenicillin (PCG) (Kikuchi *et al.* 2003) from the brain. There is also evidence to suggest that rat organic anion transporting polypeptide 2 (rOatp2: Slc21a5), another multispecific organic anion transporter expressed at the BBB (Gao *et al.* 1999), mediates efflux of amphipathic organic anions across the BBB (Asaba *et al.* 2000; Hosoya *et al.* 2000; Sugiyama *et al.* 2001; Kikuchi *et al.* 2004). Reports indicate that rOat3 mediates brain-to-blood transport of indoxyl sulfate (IS), a common uremic toxin, and that this transport is inhibited by CMPF, HA and IA (Deguchi *et al.* 2002; Ohtsuki *et al.* 2002), suggesting that rOat3 is involved in brain-to-blood transport of these toxins. Furthermore, CMPF is a substrate of rOat3 (Deguchi *et al.* 2004), which may be involved in efflux of CMPF from the brain across the BBB.

The purpose of the present study was to investigate brain-to-blood transport of CMPF, HA and IA, and to determine which transporters are involved in transport of uremic toxins at the BBB, using a *Xenopus laevis* oocyte expression system. The present results indicate that rOat3 and rOatp2 play essential roles in the efflux of CMPF, HA and IA across the BBB. The efflux clearance of each uremic toxin across the BBB was calculated using the intracerebral microinjection method, i.e. the brain efflux index (BEI), and brain slice uptake experiments. The values thus obtained were compared with influx clearance determined by *in vivo* integration plot analysis. Results of *in vivo* experiments examining the inhibitory effects of several compounds suggest that rOat3 and rOatp2 are involved in efflux processes.

Materials and methods

Materials

The full-length cDNA of rOatp2 and pGEM-HEN was donated by Dr T. Abe (Tohoku University, Sendai, Japan). CMPF was synthesized as described previously (Tsutsumi *et al.* 1999). [^{3}H]IS (2.78 Ci/mmol) and [^{3}H]CMPF (78.9 Ci/mmol) were synthesized and purified by PerkinElmer Life Sciences (Boston, MA, USA). [^{14}C]HA (55.0 mCi/mmol), [^{14}C]inulin (2.0 mCi/g) and [^{3}H]inulin (1.03 mCi/g) were purchased from American Radiolabeled Chemicals (St Louis, MO, USA). [^{3}H]IA (26.0 Ci/mmol) and [^{3}H]PCG (19.0 Ci/mmol) were obtained from Amersham Pharmacia Biotech (Little Chalfont, UK). [^{3}H]Digoxin (19.0 Ci/mmol) was purchased from PerkinElmer Life Sciences. All chemicals were of analytical grade.

Animals

Adult male Wistar rats (260–280 g) were housed in an air-conditioned room with free access to commercial feed and water, and fasted for 16 h before experiments. All animal experiments were conducted according to the guidelines of Kumamoto University for the care and use of laboratory animals.

BEI experiments

The efflux of test compounds from the brain after microinjection into the cerebral cortex was investigated using the BEI method as described previously (Kakee *et al.* 1996). The test compound ([^{3}H]CMPF, [^{14}C]HA or [^{3}H]IA) was mixed with a BBB-impermeable reference compound ([^{14}C]inulin or [^{3}H]inulin) in 0.5 μL ECF buffer (122 mM NaCl, 25 mM $NaHCO_3$, 10 mM D-glucose, 3 mM KCl, 1.4 mM $CaCl_2$, 1.2 mM $MgSO_4$, 0.4 mM K_2HPO_4, and 10 mM HEPES, pH 7.4), with or without various inhibitors at several different concentrations. Each mixture was injected into the Par2 region of a rat (0.2 mm anterior and 5.5 mm lateral to the bregma; depth 4.5 mm). The craniometric data and the precise localization of the regions to be injected were obtained from a stereotaxic atlas (Paxinos and Watson 1986). After the microinjection, the rat was decapitated, and the radioactivity in the left and right cerebrum was measured. The value 100 − BEI (%), which represents the percentage of the test compound remaining in the cerebrum, was calculated using equation 1.

$$100 - \mathrm{BEI}(\%) = \frac{\dfrac{\text{Amount of test compound in the brain}}{\text{Amount of reference in the brain}}}{\dfrac{\text{Amount of test compound injectate}}{\text{Amount of reference injectate}}} \quad (1)$$

The apparent brain efflux rate constant across the BBB (K_{eff}) was obtained by fitting the value of 100 − BEI (%) to the time data, using a non-linear least-squares regression program (MULTI) (Yamaoka *et al.* 1981).

The apparent efflux clearance across the BBB, $CL_{BBB,eff}$, was calculated using equation 2.

$$CL_{BBB,eff} = K_{\mathrm{eff}} \times V_{d,brain} \quad (2)$$

where $V_{d,brain}$ represents the distribution volume of test compounds in the brain, as determined in the *in vitro* brain slice uptake experiment, as described previously (Kakee *et al.* 1996).

In vivo integration plot analysis

The apparent influx clearance of test compounds in the cerebrum after intravenous administration was determined by performing integration plot analysis as described previously (Kakee *et al.* 1996). Each test compound ([^{3}H]CMPF, [^{14}C]HA, [^{3}H]IA or [^{3}H]IS; 5 μCi/kg) was administered intravenously via a left femoral vein. After plasma samples had been drawn from the femoral artery at the designated times, rats were decapitated at 1, 2, 3, 5 or 60 min. The radioactivity in the left and right cerebrum was measured. The brain influx rate of test compounds was calculated using the following differential equation:

$$\frac{dX_t}{dt} = CL_{brain,inf} \times C_p \quad (3)$$

where X_t is the amount of the test compound in the cerebrum at time t, $CL_{brain,inf}$ is the apparent influx clearance in the cerebrum, and C_p is the plasma concentration of the test compound. Integration of equation 3 yields the following equation:

$$X_t = CL_{brain,inf} \times AUC_{0-t} + C_p \times V_0 \quad (4)$$

where AUC_{0-t} represents the area under the plasma concentration time curve from time 0 to t, and V_0 is the capillary space in the brain. Dividing equation 4 by C_p yields the following equation:

$$\frac{X_p}{C_p} = \frac{CL_{brain,inf} \times AUC_{0-t}}{C_p} + V_0 \quad (5)$$

Thus, the value $CL_{brain,inf}$ can be obtained from the initial slope of a plot of X_t/C_p versus AUC_{0-t}/C_p, which is designated here as the 'integration plot'.

Expression of rOat3 and rOatp2 in *X. laevis* oocytes

Using T7 RNA polymerase, capped cRNAs were transcribed from *Not*I-linearized pGEM-HEN vector containing rOat3 and rOatp2 cDNA, as described elsewhere (Deguchi *et al.* 2002). Defolliculated oocytes were injected with 50 nL water or the capped cRNAs (15 ng), and incubated in freshly prepared Barth's solution (88 mM NaCl, 1 mM KCl, 0.33 mM $Ca(NO_3)_2$, 0.4 mM $CaCl_2$, 0.8 mM $MgSO_4$, 2.4 mm $NaHCO_3$, 10 mm HEPES, pH 7.4) containing 50 μg/mL gentamicin and 2.5 mM pyruvate at 18°C. The Barth's solution used to incubate the oocytes was replaced with fresh solution daily. Uptake experiments were performed after incubation for 3 days.

Uptake by *X. laevis* oocytes

Before the uptake experiment, oocytes were preincubated with 500 μL ND96 solution (96 mM NaCl, 2 mM KCl, 1.8 mM $CaCl_2$, 1 mM $MgCl_2$, 5 mM HEPES, pH 7.4) for 20 min at 20°C. At the beginning of the uptake experiment, the original ND96 solution was replaced with 200 μL ND96 solution containing one of the following test compounds: 1 μM [^{3}H]CMPF (0.3 μCi), 1 μM [^{3}H]IA (0.3 μCi), 1 μM [^{3}H]PCG (0.3 μCi), 1 μM [^{3}H]digoxin (0.3 μCi) or 10 μM [^{14}C]HA (0.1 μCi). After incubation for the designated time at 20°C, the uptake experiment was terminated by adding ice-cold ND96 solution. Oocytes were then washed four times with ice-cold ND96 solution and solubilized in 5% sodium dodecyl sulfate solution, and the accumulated radioactivity was measured using a liquid scintillation counter.

In the inhibition experiment, we measured uptake of radiolabeled test compounds by rOat3 or rOatp2 in the presence or absence of various unlabeled compounds in ND96 solution. Specific uptake was calculated by subtracting uptake by water-injected oocytes from uptake by oocytes expressing rOat3 or rOatp2.

Kinetic analysis

Kinetic parameters were calculated using the Michaelis–Menten equation:

$$v = \frac{V_{max} \times S}{K_m + S} + CL_{non} \times S \quad (6)$$

where v is the uptake velocity (or the efflux transport velocity at the BBB) of the substrate, S is the substrate concentration in the medium (or injected solution), K_m is the Michaelis–Menten constant, V_{max} is the maximum uptake rate (or the maximum efflux transport rate at the BBB), and CL_{non} is the non-saturable transport clearance. Inhibition constants (K_i values) of a series of compounds were determined by examining their inhibitory effects on rOat3- and rOatp2-mediated uptake, assuming competitive inhibition with a substrate concentration much lower than the K_m of the substrate, using the following equation:

$$CL_{+I} = \frac{CL}{1 + I/K_i} \quad (7)$$

where CL represents uptake clearance, I represents concentration of the inhibitor, and the subscript + I indicates CL in the presence of the inhibitor. In the inhibition experiment, the substrate concentration was low, compared with the K_m of the substrate. Fitting was performed using the non-linear least-squares method, a MULTI program (Yamaoka *et al.* 1981) and the Damping Gauss Newton Method algorithm.

Statistical analysis

Unless otherwise indicated, data are presented as mean ± SEM; the SEM value was used to indicate the confidence limits of mean values calculated from each observed value. Values for kinetic parameters are presented as mean ± SD, based on calculation using the iterative non-linear least-squares regression analysis program MULTI; the SD value indicates the variance of each parameter based on the observed values. An unpaired, two-tailed Student's *t*-test was used to assess the significance of differences between means of two groups. One-way ANOVA followed by the modified Fisher's least-squares difference method was used to assess the statistical significance of differences between means of more than two groups.

Results

Efflux of uremic toxins from the brain across the BBB

The time profiles of the efflux of [^{3}H]CMPF, [^{14}C]HA and [^{3}H]IA from the brain after microinjection into the cerebral cortex are shown in Fig. 1. Uremic toxins were transported from the brain into the systemic circulation, and their efflux showed linearity up to 40 min following microinjection. Mean ± SD K_{eff} was calculated as $3.93 \times 10^{-2} \pm 0.22 \times$

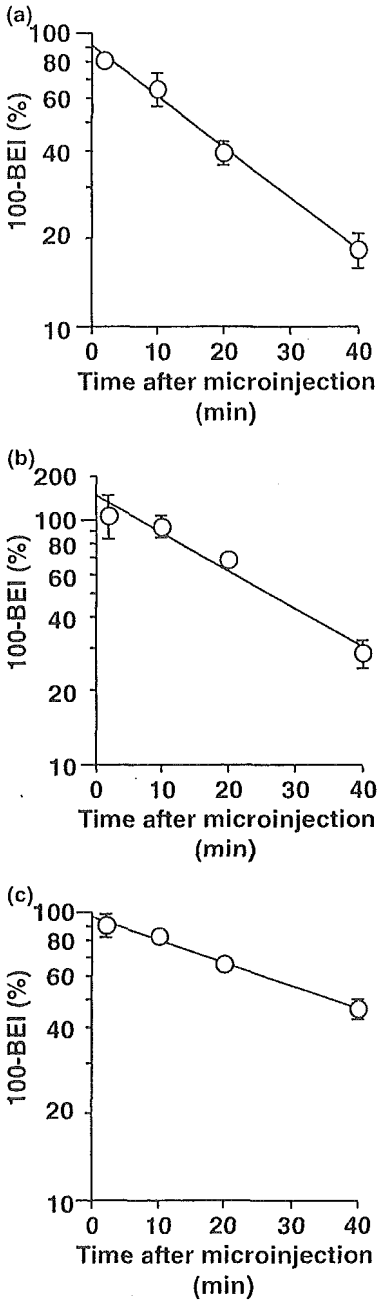

Fig. 1 Time profile of [^{3}H]CMPF (a), [^{14}C]HA (b) and [^{3}H]IA (c) in the cerebrum after intracerebral microinjection. A mixture of [^{3}H]CMPF (50 nCi/rat) or [^{3}H]IA (50 nCi/rat) and [^{14}C]inulin (5 nCi/rat), or [^{14}C]HA (20 nCi/rat) and [^{3}H]inulin (100 nCi/rat) dissolved in 0.5 μL ECF buffer was injected into Par2 of the rat cerebrum; animals were then decapitated at designated times. The solid line represents the fitted value obtained by non-linear regression analysis. Values are mean ± SEM (n = 4–7).

10^{-2} per min for CMPF, $3.54 \times 10^{-2} \pm 0.41 \times 10^{-2}$ per min for HA, and $1.79 \times 10^{-2} \pm 0.05 \times 10^{-2}$ per min for IA (Table 1).

Comparison between efflux and influx clearance of uremic toxins at the BBB

The distribution volume of uremic toxins in the brain, $V_{d,brain}$, was determined in the *in vitro* brain slice uptake experiment. There was no significant difference in the slice-to-medium concentration ratio (S/M ratio) among [^{3}H]CMPF, [^{14}C]HA, [^{3}H]IA and [^{3}H]IS, for incubation periods of 60–120 min. The mean ± SD steady-state S/M ratios ($V_{d,brain}$) of [^{3}H]CMPF, [^{14}C]HA, [^{3}H]IA and [^{3}H]IS were 0.75 ± 0.02, 0.92 ± 0.08, 1.02 ± 0.12 and 1.17 ± 0.07 mL/g brain respectively (Table 1). The apparent efflux clearance of uremic toxins across the BBB ($CL_{BBB,eff}$) was calculated by multiplying K_{eff} by $V_{d,brain}$. The mean ± SD efflux clearances of CMPF, HA, IA and IS were 29.7 ± 1.8, 32.7 ± 4.8, 18.2 ± 2.3 and 12.6 ± 2.0 μL/min/g brain respectively (Table 1).

The influx clearance of uremic toxins across the BBB was determined using an *in vivo* integration plot analysis (Table 1). The mean ± SD influx clearances of [^{3}H]CMPF, [^{14}C]HA, [^{3}H]IA and [^{3}H]IS across the BBB were 3.76 ± 0.71, 2.71 ± 0.55, 8.83 ± 1.69 and 4.81 ± 0.38 μL/min/g brain respectively. These toxins show high plasma protein binding (Sakai *et al.* 1996; Tsutsumi *et al.* 2002) so the effective concentration of the toxin may be decreased in circulation owing to protein binding. For all uremic toxins tested, the apparent efflux clearance across the BBB was greater than the estimated influx clearance.

Concentration-dependent efflux of uremic toxins from the brain

To characterize the efflux transport system at the BBB, we calculated K_{eff} in the presence or absence of inhibitors, using the 100 − BEI (%) data obtained at 2 and 20 min for [^{3}H]CMPF and [^{14}C]HA. Because of lower efflux rate, the K_{eff} of [^{3}H]IA was determined from the data at 2 and 40 min. K_{eff} values of [^{3}H]CMPF, [^{14}C]HA and [^{3}H]IA decreased with increasing concentration of unlabeled substrate in the injectate (Fig. 2). The magnitude of the dilution factor determines the concentration of the toxin in the cerebrum and markedly influences the asymmetry of transport. Given a dilution factor of 46.2 in the cerebrum after intracerebral microinjection (Kakee *et al.* 1996), the apparent K_m for the efflux of CMPF, HA and IA from the brain across the BBB was estimated as 28.7 ± 9.9, 21.9 ± 10.3 and 355 ± 29 μM respectively. Approximately 70% of the non-saturable efflux of IA was maintained even with 300 mM unlabeled IA in the injection solution (Fig. 2c); this remaining fraction may be attributed to a low-affinity transport system or passive diffusion.

Effect of inhibitors on efflux of uremic toxins across the BBB

The inhibitors shown in Table 2 were injected into rat brains along with radiolabeled uremic toxins. The organic anions

Table 1 Comparison between influx and efflux clearance of uremic toxins across the BBB

Uremic toxins	K_{eff} (x 10^{-2} per min)	$V_{d,brain}$ (mL/g brain)	$CL_{BBB,eff}$ (μL/min/g brain)	$CL_{brain,inf}$ (μL/min/g brain)	Efflux/Influx (fold)
CMPF	3.93 ± 0.22	0.75 ± 0.02	29.7 ± 1.8	3.76 ± 0.71	7.9
HA	3.54 ± 0.41	0.92 ± 0.08	32.7 ± 4.8	2.71 ± 0.55	12
IA	1.79 ± 0.05	1.02 ± 0.12	18.2 ± 2.3	8.83 ± 1.69	2.1
IS	1.08 ± 0.16[a]	1.17 ± 0.07	12.6 ± 2.0	4.81 ± 0.38	2.6

Values are mean ± SD ($n = 3$). [a]From Ohtsuki *et al.* (2002).

probenecid, PAH and PCG significantly inhibited efflux transport of uremic toxins in a concentration-dependent manner. Taurocholate reduced the efflux transport of [^{3}H]CMPF in a concentration-dependent fashion, and 100 mM taurocholate significantly inhibited efflux of [^{14}C]HA. However, taurocholate did not significantly inhibit efflux of [^{3}H]IA. Digoxin, a specific inhibitor of rOatp2, significantly inhibited efflux transport of [^{3}H]CMPF by about 30%.

Uptake of uremic toxins by rOat3- or rOatp2-expressing *X. laevis* oocytes

The activity of rOat3- and rOatp2-expressing oocytes was confirmed by the observed transport of [^{3}H]PCG and [^{3}H]digoxin, which are typical substrates of rOat3 and rOatp2 respectively (Fig. 3). The oocytes injected with rOat3 cRNA exhibited about 28-fold greater uptake of [^{3}H]PCG than oocytes injected with water. Oocytes injected with rOatp2 cRNA exhibited about 7-fold greater uptake of [^{3}H]digoxin than oocytes injected with water, and rOatp2-mediated [^{3}H]digoxin uptake was linear over a period of at least 60 min (data not shown). The amount of [^{3}H]CMPF taken up by oocytes injected with rOat3 or rOatp2 cRNA was significantly greater than that of oocytes injected with water. The rOat3-mediated [^{3}H]CMPF uptake was linear over a period of at least 120 min (data not shown). Specific uptake of [^{3}H]CMPF by rOAT3-expressing oocytes revealed saturable kinetics, and the estimated mean ± SD K_m and V_{max} values were 6.43 ± 0.90 μM and 7.28 ± 0.68 pmol/h/oocyte respectively. There was a significant difference in uptake of [^{14}C]HA and [^{3}H]IA between rOat3-expressing oocytes and oocytes injected with water, whereas there was no significant difference over a period of at least 60 min in uptake of [^{14}C]HA or [^{3}H]IA between oocytes injected with rOatp2 cRNA and those injected with water.

To examine the possibility that uremic toxins are involved in rOatp2-mediated transport, we analyzed the affinities of uremic toxins for rOatp2. Because we did not observe marked uptake of CMPF or significant uptake of HA or IA by rOatp2-expressing oocytes, the K_i values for rOatp2 in those oocytes were calculated using the uptake of [^{3}H]digoxin at 60 min (Fig. 4). The K_i values obtained assuming competitive inhibition are summarized in Table 3. CMPF and IS inhibited transport via rOatp2, but they exhibited lower affinity for rOatp2 than for rOat3. HA and IA inhibited transport via rOat3, but did not inhibit uptake via rOatp2. An increase in [^{3}H]digoxin uptake at low concentrations of IS and HA was observed. Further kinetic studies are needed to describe the allosteric interaction between substrate and inhibitor.

Discussion

The *in vivo* data obtained in the present study show that CMPF, HA and IA, which are anionic uremic toxins, are transported via carrier-mediated efflux transport from brain tissue to the bloodstream across the BBB. Approximately 80, 70 and 55% of the administered dose of [^{3}H]CMPF, [^{14}C]HA and [^{3}H]IA respectively was eliminated from the cerebrum into the systemic circulation within 40 min (Fig. 1). For all uremic toxins tested, the apparent efflux clearance across the BBB (calculated by multiplying the elimination rate constant by the distribution volume in the brain) was greater than the apparent influx clearance, suggesting that brain concentrations of uremic toxins are dependent on their efflux transport across the BBB. The lower brain distribution of these uremic toxins may be partly due to their greater efflux clearance from the brain; another possible cause is their lower uptake clearance from the blood circulation, because they are more highly bound to plasma proteins (Sakai *et al.* 1996; Tsutsumi *et al.* 2002). These results also suggest that these uremic toxins are asymmetrically transported across the BBB.

Efflux transport of [^{3}H]CMPF, [^{14}C]HA and [^{3}H]IA was saturable, with a K_m of 28.7, 21.9 and 355 μM respectively for cerebral concentration (Fig. 2). The results indicate that these uremic toxins undergo carrier-mediated efflux transport across the BBB. The results therefore suggest that BBB efflux transport systems for these three uremic toxins play a key role (as a detoxifying system) in reducing levels of these toxins in brain interstitial fluid.

To examine characteristics of the transporters involved in the efflux of CMPF, HA and IA, inhibition experiments were performed *in vivo* using the BEI method. Saturable efflux of [^{3}H]CMPF, [^{14}C]HA and [^{3}H]IA from the brain was almost completely inhibited by simultaneous injection of probenecid (Table 2). In previous studies, PAH and PCG (Sugiyama *et al.* 2001; Kikuchi *et al.* 2003) have been used as selective inhibitors of efflux transport of hydrophilic organic anions

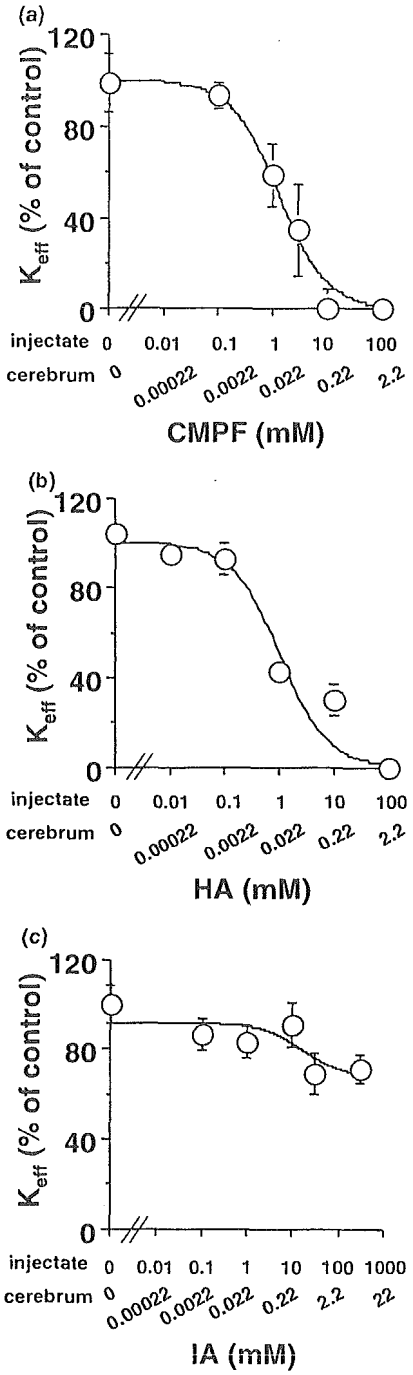

Fig. 2 Concentration dependence of the efflux of uremic toxins across the BBB. (a) A mixture of [^{3}H]CMPF and [^{14}C]inulin dissolved in ECF buffer was injected into Par2 with 0, 0.1, 1, 3, 10 or 100 mM unlabeled CMPF in the injectate. Rats were decapitated 20 min after microinjection, and the elimination rate constant was calculated. (b) A mixture of [^{14}C]HA and [^{3}H]inulin dissolved in saline was injected intracerebrally with 0, 0.01, 0.1, 1, 10 or 100 mM unlabeled HA in the injectate. Rats were decapitated 20 min after microinjection, and the elimination rate constant was determined. (c) A mixture of [^{3}H]IA and [^{14}C]inulin dissolved in saline was injected intracerebrally with 0, 0.1, 1, 10, 30 or 300 mM unlabeled IA in the injectate. Rats were decapitated 40 min after microinjection, and the elimination rate constant was determined. Each value of cerebral concentration was estimated by dividing the concentration in the injectate by the dilution factor of 46.2 (Kakee *et al.* 1996). The solid lines represent the fitted line obtained by non-linear regression analysis. Values are mean ± SEM (n = 3–8).

across the BBB, and taurocholate and digoxin (Sugiyama *et al.* 2001; Kikuchi *et al.* 2004) have been used as selective inhibitors of efflux transport of amphipathic organic anions across the BBB. The efflux of each of the present uremic toxins was inhibited by these inhibitors in a concentration-dependent manner (Table 2). PCG completely inhibited the saturable efflux of [^{3}H]CMPF, [^{14}C]HA and [^{3}H]IA, whereas the maximum inhibitory effect of PAH differed significantly between [^{14}C]HA and other uremic toxins. PAH completely inhibited the saturable efflux of [^{3}H]CMPF and [^{3}H]IA, but only partially inhibited the efflux of [^{14}C]HA, suggesting that these toxins are not all transported by the same transporters. Taurocholate only partially inhibited the efflux of [^{3}H]CMPF and [^{14}C]HA (by 65% and 70% respectively), even at concentrations sufficient to saturate efflux (Kitazawa *et al.* 1998; Sugiyama *et al.* 2001). Digoxin inhibited the efflux of [^{3}H]CMPF by 30%. These results suggest that the efflux of uremic toxins occurs via PAH-, PCG-, taurocholate- and digoxin-sensitive pathways.

PAH and PCG have been used as inhibitors of rOat3 (Kikuchi *et al.* 2003). Taurocholate has been used as an inhibitor of amphipathic organic anion transport systems, including rOatp2, and digoxin is a specific inhibitor of rOatp2 (Sugiyama *et al.* 2001). In the present study, the saturable efflux transport of [^{14}C]HA and [^{3}H]IA from the brain was markedly inhibited by PAH and PCG, whereas taurocholate did not inhibit efflux of [^{14}C]HA or [^{3}H]IA at the concentration selective for amphipathic organic anion transport systems. This suggests that efflux of HA and IA from the brain to the bloodstream across the BBB is mediated by rOat3. The finding that efflux of [^{14}C]HA was completely inhibited by PCG and partially inhibited by PAH suggests that PCG-sensitive, PAH-resistant transporters are involved in the efflux of HA. Thus, the present results suggest that rOat3 and PCG-sensitive, PAH-resistant transporters mediate the efflux transport of HA across the BBB. The efflux transport of [^{3}H]CMPF was inhibited to a greater degree by PAH and PCG than by taurocholate or digoxin (Table 2). Although a higher concentration of digoxin was not achieved owing to its limited solubility (Table 2), the kinetic parameters for digoxin (K_i 37 nM for rOatp2) (Sugiyama *et al.* 2001) indicated that 0.1 mM digoxin should saturate rOatp2-mediated transport. Assuming that the PAH- and PCG-sensitive fraction of the efflux of [^{3}H]CMPF represents the contribution of rOat3, and that the digoxin-sensitive fraction represents the contribution of rOatp2, it appears that rOat3 is the primary mediator of the efflux of CMPF across the BBB,

Table 2 Inhibitory effects of organic anions for the efflux transport of radiolabeled uremic toxins across the BBB

Inhibitors	Injected concentration (mM)	Cerebral concentration (μM)	% of control		
			[^{3}H]CMPF	[^{14}C]HA	[^{3}H]IA
Control	–	–	100 ± 12 (5)	100 ± 8 (4)	100 ± 12 (7)
Probenecid	100	2165	3.24 ± 2.94 (3)**	8.45 ± 1.21 (3)**	69.1 ± 9.3 (6)*
PAH	10	216	37.0 ± 9.7 (3)**	68.0 ± 6.0 (7)*	69.0 ± 6.4 (4)*
	100	2165	4.60 ± 6.79 (3)**	70.4 ± 4.1 (16)*	64.1 ± 5.0 (3)*
PCG	10	216	7.73 ± 5.32 (5)**	43.6 ± 20.9 (6)**	–
	100	2165	0.34 ± 0.34 (3)**	− 21.7 ± 4.0 (3)**	70.1 ± 8.0 (8)**
Taurocholate	10	216	44.8 ± 3.0 (4)**	94.8 ± 6.6 (3)	–
	100	2165	33.9 ± 17.7 (3)**	29.9 ± 6.8 (9)**	90.4 ± 0.6 (3)
Digoxin	0.1	2.16	70.5 ± 6.2 (7)**	92.5 ± 4.5 (4)	–

ECF buffer containing [^{3}H]radiolabeled test compounds ([^{3}H]CMPF or [^{3}H]IA, 50 nCi/rat) and [^{14}C]inulin (5 nCi/rat), or [^{14}C]HA (20 nCi/rat) and [^{3}H]inulin (100 nCi/rat), with or without unlabeled inhibitors was microinjected into Par2 of rat cerebrum, and the apparent brain efflux rate constant across the BBB (K_{eff}) of radiolabeled uremic toxins was determined. Each value of the cerebral concentration was estimated by the concentration in the injectate divided by the dilution factor of 46.2 (Kakee *et al.* 1996). Results are given as a ratio with respect to K_{eff} determined in the absence of unlabeled inhibitors. Values are mean ± SEM (*n* is given in parentheses). *$p < 0.05$, **$p < 0.01$, significantly different from corresponding control value. Statistical analysis was performed by ANOVA.

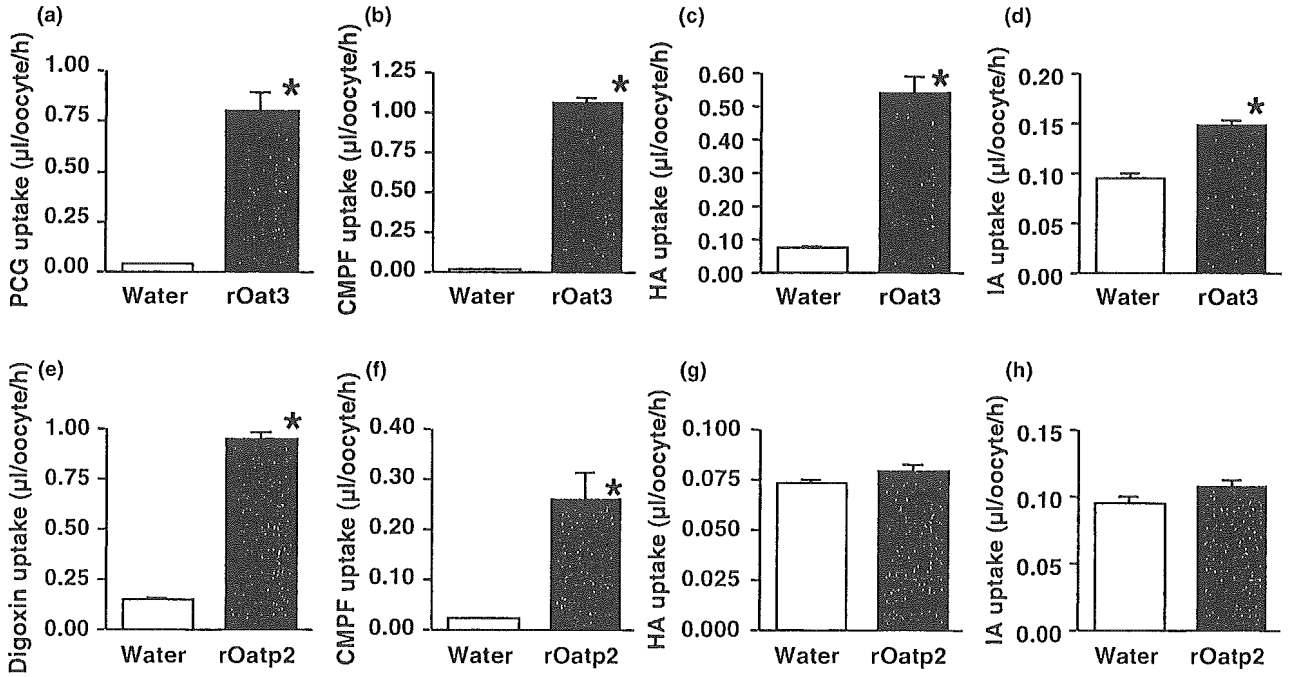

Fig. 3 rOat3-mediated (a–d) and rOatp2-mediated (e–h) uptake of radiolabeled compounds. The uptake of radiolabeled compounds ([^{3}H]PCG [a; 1 μM], [^{3}H]digoxin [e; 1 μM], [^{3}H]CMPF [b and f; 1 μM], [^{3}H]IA [d and h; 1 μM] and [^{14}C]HA [c and g; 10 μM]) by *X. laevis* oocytes injected with water or rOat3 or rOatp2 cRNA was measured after incubation for 1 h. Values are mean ± SEM; $n = 10$–20. *$p < 0.01$, significantly different from uptake by oocytes injected with water. Statistical analysis was performed by Student's *t*-test.

and that rOatp2 is also involved. The sum of the degree of inhibition of the efflux of [^{3}H]CMPF by selective inhibitors exceeded 100% at the concentration selective for each transporter. It is likely that the selective inhibitors inhibit other transporters at the BBB, including those expressed on the luminal membrane, because the net efflux across the BBB was evaluated using the BEI method.

The inhibitory effect shown in Table 2 suggests the involvement of rOat3 and rOatp2 in transport of uremic toxins at the BBB. The results of the transport experiments using the

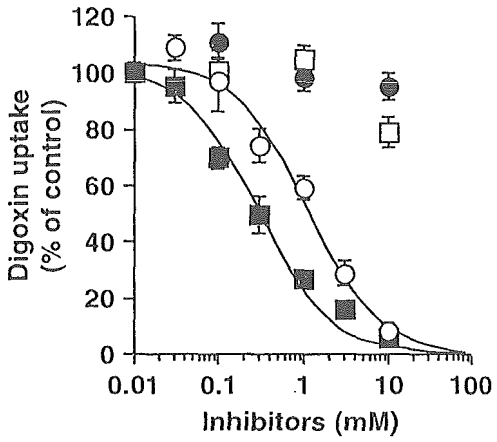

Fig. 4 Inhibition profile of rOatp2-mediated [^{3}H]digoxin uptake in the presence of CMPF (■), IS (○), HA (●) or IA (□). Values are expressed as a percentage of [^{3}H]digoxin uptake in rOatp2-expressing oocytes at 1 h in the absence of inhibitor. Values are mean ± SEM; n = 8–12.

Table 3 Kinetic parameters of uremic toxins determined by BEI method, or in rOat3 and rOatp2 expression systems

Uremic toxins	K_m or K_i (μM)		
	BEI	rOat3	rOatp2
CMPF	K_m = 28.7 ± 9.9	K_m = 6.43 ± 0.90 K_m = 10.9 ± 2.0[c]	K_i = 301 ± 51
HA	K_m = 21.9 ± 10.3	K_i = 11.9 ± 2.6[a] K_i = 18.6 ± 10.7[c]	K_i > 10 000
IA	K_m = 355 ± 29	K_i = 509 ± 96[a] K_i = 582 ± 113[c]	K_i > 10 000
IS	K_m = 298 ± 43[b]	K_m = 158 ± 0.1[a]	K_i = 1105 ± 190

Values are mean ± SD (n = 3–12). [a]From Deguchi *et al.* (2002); [b]from Ohtsuki *et al.* (2002); [c]from Deguchi *et al.* (2004).

X. laevis oocyte expression system indicate that CMPF is a substrate of both rOat3 and rOatp2 (Figs 3b and f). Correcting the uptake of [^{3}H]PCG and [^{3}H]CMPF in rOat3-expressing oocytes by the respective uptake in water-injected controls revealed that [^{3}H]CMPF is much better translocated than [^{3}H]PCG (Figs 3a and b). The uptake clearance of [^{3}H]digoxin in rOatp2-expressing oocytes was 3.4 times greater than that of [^{3}H]CMPF. The results also indicate that [^{14}C]HA and [^{3}H]IA are substrates of rOat3 (Figs 3c and d), although their uptake clearance was several times lower than that of [^{3}H]PCG. These results suggest that rOat3 and/or rOatp2 are involved in the efflux of uremic toxins from the brain across the BBB. Furthermore, the apparent K_m values of the efflux of CMPF, HA and IA were comparable to their respective K_m values for rOat3 (Table 3). These results suggest that rOat3 plays an important role in the efflux transport of these uremic toxins across the barriers of the CNS.

Under uremic conditions, serum levels of CMPF, HA and IA reportedly increase from their normal values (< 32 μM, < 28 μM and < 0.1 μM respectively) to 390 μM, 2.6 mM and 52 μM respectively (Saito *et al.* 1996; Vanholder *et al.* 2003), and the level of HA in the brain has been shown to increase from its normal value (11 μM) to 42 μM (Porter *et al.* 1975). The K_m value of HA transport at the BBB (22 μM; Table 3) was comparable with the brain concentration in chronic renal failure, so accumulation of uremic toxins, particularly HA, in uremic patients may reduce brain-to-blood transport by rOat3 and/or rOatp2 at the BBB. Recent reports indicate that IS, which is a typical uremic toxin, evokes significant whole-cell currents, suggesting that IS affects miscellaneous membrane ionic conductances, probably involving voltage-gated Ca^{2+} channels (D'Hooge *et al.* 2003). It was previously demonstrated that rOat3 mediates the brain-to-blood transport of IS (Ohtsuki *et al.* 2002). In the present study, the apparent efflux clearance of IS across the BBB was greater than its influx clearance (Table 1). In addition, the apparent K_m value of the efflux of IS was comparable to the K_m value of rOat3, but was not comparable to the K_m value of rOatp2 (Table 3). These results indicate that rOat3 plays an important role in the efflux transport of IS across the BBB. Ohtsuki *et al.* (2002) also suggested that inhibition of rOat3-mediated brain-to-blood transport by uremic toxins leads to accumulation of neurotransmitter metabolites and drugs in the brain of uremic patients. Although it is not known whether uremic neurotoxins including IS and neurotransmitter metabolites have severe neurotoxic effects, the present findings highlight the importance of carrier-mediated transport of uremic toxins across the BBB, and help clarify the mechanisms of neurological symptoms of uremic syndrome in patients with chronic renal failure.

In conclusion, CMPF, HA and IA undergo efflux from the brain into the blood across the BBB, and at least two transporters (rOat3 and/or rOatp2) are involved in their efflux. Efflux transport of these toxins across the BBB appears to involve interaction with neurotransmitter metabolites and uremic neurotoxins. The present findings provide a molecular basis for this phenomenon, and help clarify the pathophysiological functions of the BBB as a detoxifying system under normal and uremic conditions.

Acknowledgements

We would like to thank Dr T. Abe for supplying the full-length cDNA of rOatp2 and the pGEM-HEN vector for protein expression in *X. laevis* oocytes. This work was supported, in part, by the Sasakawa Scientific Research Grant from The Japan Science Society.

References

Asaba H., Hosoya K., Takanaga H., Ohtsuki S., Tamura E., Takizawa T. and Terasaki T. (2000) Blood–brain barrier is involved in the efflux

transport of a neuroactive steroid, dehydroepiandrosterone sulfate, via organic anion transporting polypeptide 2. *J. Neurochem.* **75**, 1907–1916.

Brouns R. and De Deyn P. P. (2004) Neurological complications in renal failure: a review. *Clin. Neurol. Neurosurg.* **107**, 1–16.

Costigan M. G., Callaghan C. A. and Lindup W. E. (1996) Hypothesis: is accumulation of a furan dicarboxylic acid (3-carboxy-4-methyl-5-propyl-2-furanpropanoic acid) related to the neurological abnormalities in patients with renal failure? *Nephron* **73**, 169–173.

D'Hooge R., Van de Vijver G., Van Bogaert P. P., Marescau B., Vanholder R. and De Deyn P. P. (2003) Involvement of voltage- and ligand-gated Ca^{2+} channels in the neuroexcitatory and synergistic effects of putative uremic neurotoxins. *Kidney Int.* **63**, 1764–1775.

Deguchi T., Ohtsuki S., Otagiri M., Takanaga H., Asaba H., Mori S. and Terasaki T. (2002) Major role of organic anion transporter 3 in the transport of indoxyl sulfate in the kidney. *Kidney Int.* **61**, 1760–1768.

Deguchi T., Kusuhara H., Takadate A., Endou H., Otagiri M. and Sugiyama Y. (2004) Characterization of uremic toxin transport by organic anion transporters in the kidney. *Kidney Int.* **65**, 162–174.

Gao B., Stieger B., Noe B., Fritschy J. M. and Meier P. J. (1999) Localization of the organic anion transporting polypeptide 2 (Oatp2) in capillary endothelium and choroid plexus epithelium of rat brain. *J. Histochem. Cytochem.* **47**, 1255–1264.

Hosoya K., Asaba H. and Terasaki T. (2000) Brain-to-blood efflux transport of estrone-3-sulfate at the blood–brain barrier in rats. *Life Sci.* **67**, 2699–2711.

Kakee A., Terasaki T. and Sugiyama Y. (1996) Brain efflux index as a novel method of analyzing efflux transport at the blood–brain barrier. *J. Pharmacol. Exp. Ther.* **277**, 1550–1559.

Kikuchi R., Kusuhara H., Sugiyama D. and Sugiyama Y. (2003) Contribution of organic anion transporter 3 (Slc22a8) to the elimination of *p*-aminohippuric acid and benzylpenicillin across the blood–brain barrier. *J. Pharmacol. Exp. Ther.* **306**, 51–58.

Kikuchi R., Kusuhara H., Abe T., Endou H. and Sugiyama Y. (2004) Involvement of multiple transporters in the efflux of 3-hydroxy-3-methylglutaryl-CoA reductase inhibitors across the blood–brain barrier. *J. Pharmacol. Exp. Ther.* **311**, 1147–1153.

Kitazawa T., Terasaki T., Suzuki H., Kakee A. and Sugiyama Y. (1998) Efflux of taurocholic acid across the blood–brain barrier: interaction with cyclic peptides. *J. Pharmacol. Exp. Ther.* **286**, 890–895.

Kusuhara H. and Sugiyama Y. (2001a) Efflux transport systems for drugs at the blood–brain barrier and blood–cerebrospinal fluid barrier (Part 1). *Drug Discov. Today* **6**, 150–156.

Kusuhara H. and Sugiyama Y. (2001b) Efflux transport systems for drugs at the blood–brain barrier and blood–cerebrospinal fluid barrier (Part 2). *Drug Discov. Today* **6**, 206–212.

Loscher W. and Potschka H. (2005) Blood–brain barrier active efflux transporters: ATP-binding cassette gene family. *Neurorx* **2**, 86–98.

Moe S. M. and Sprague S. M. (1994) Uremic encephalopathy. *Clin. Nephrol.* **42**, 251–256.

Mori S., Takanaga H., Ohtsuki S., Deguchi T., Kang Y. S., Hosoya K. and Terasaki T. (2003) Rat organic anion transporter 3 (rOAT3) is responsible for brain-to-blood efflux of homovanillic acid at the abluminal membrane of brain capillary endothelial cells. *J. Cereb. Blood Flow Metab.* **23**, 432–440.

Mori S., Ohtsuki S., Takanaga H., Kikkawa T., Kang Y. S. and Terasaki T. (2004) Organic anion transporter 3 is involved in the brain-to-blood efflux transport of thiopurine nucleobase analogs. *J. Neurochem.* **90**, 931–941.

Muting D. (1965) Studies on the pathogenesis of uremia. Comparative determinations of glucuronic acid, indican, free and bound phenols in the serum, cerebrospinal fluid, and urine of renal diseases with and without uremia. *Clin. Chim. Acta* **12**, 551–554.

Niwa T. (1996) Organic acids and the uremic syndrome: protein metabolite hypothesis in the progression of chronic renal failure. *Semin. Nephrol.* **16**, 167–182.

Ohtsuki S., Asaba H., Takanaga H., Deguchi T., Hosoya K., Otagiri M. and Terasaki T. (2002) Role of blood–brain barrier organic anion transporter 3 (OAT3) in the efflux of indoxyl sulfate, a uremic toxin: its involvement in neurotransmitter metabolite clearance from the brain. *J. Neurochem.* **83**, 57–66.

Pardridge W. M. (1999) Blood–brain barrier biology and methodology. *J. Neurovirol.* **5**, 556–569.

Paxinos G. and Watson C. (1986) *The Rat Brain in Stereotaxic Coordinates*. Academic Press, New York.

Porter R. D., Cathcart-Rake W. F., Wan S. H., Whittier F. C. and Grantham J. J. (1975) Secretory activity and aryl acid content of serum, urine, and cerebrospinal fluid in normal and uremic man. *J. Lab. Clin. Med.* **85**, 723–731.

Saito H., Masuda S. and Inui K. (1996) Cloning and functional characterization of a novel rat organic anion transporter mediating basolateral uptake of methotrexate in the kidney. *J. Biol. Chem.* **271**, 20719–20725.

Sakai T., Maruyama T., Imamura H., Shimada H. and Otagiri M. (1996) Mechanism of stereoselective serum binding of ketoprofen after hemodialysis. *J. Pharmacol. Exp. Ther.* **278**, 786–792.

Schoots A. C., De Vries P. M., Thiemann R., Hazejager W. A., Visser S. L. and Oe P. L. (1989) Biochemical and neurophysiological parameters in hemodialyzed patients with chronic renal failure. *Clin. Chim. Acta* **185**, 91–107.

Smogorzewski M. J. (2001) Central nervous dysfunction in uremia. *Am. J. Kidney Dis.* **38**, S122–S128.

Sugiyama D., Kusuhara H., Shitara Y., Abe T., Meier P. J., Sekine T., Endou H., Suzuki H. and Sugiyama Y. (2001) Characterization of the efflux transport of 17beta-estradiol-D-17beta-glucuronide from the brain across the blood–brain barrier. *J. Pharmacol. Exp. Ther.* **298**, 316–322.

Tsutsumi Y., Maruyama T., Takadate A., Goto M., Matsunaga H. and Otagiri M. (1999) Interaction between two dicarboxylate endogenous substances, bilirubin and an uremic toxin, 3-carboxy-4-methyl-5-propyl-2-furanpropanoic acid, on human serum albumin. *Pharm. Res.* **16**, 916–923.

Tsutsumi Y., Deguchi T., Takano M., Takadate A., Lindup W. E. and Otagiri M. (2002) Renal disposition of a furan dicarboxylic acid and other uremic toxins in the rat. *J. Pharmacol. Exp. Ther.* **303**, 880–887.

Vanholder R., De Smet R., Glorieux G. *et al.* (2003) Review on uremic toxins: classification, concentration, and interindividual variability. *Kidney Int.* **63**, 1934–1943.

Yamaoka K., Tanigawara Y., Nakagawa T. and Uno T. (1981) A pharmacokinetic analysis program (multi) for microcomputer. *J. Pharmacobiodyn.* **4**, 879–885.

